Prediction of Land Use Changes and Flood Risk Maps Using GIS and ANN Modelling in Perak

by

Nurul Balkhis Athirah binti Kamaruzaman
17002461

Dissertation submitted in partial fulfillment of
the requirements for the
Bachelor of Civil Engineering with Honours

JANUARY 2022

Universiti Teknologi PETRONAS
Bandar Seri Iskandar
32610
Perak Darul Ridzuan

CERTIFICATION OF APPROVAL

Prediction of Land Use Changes and Flood Risk Maps Using GIS and ANN Modelling in Perak

by

Nurul Balkhis Athirah binti Kamaruzaman

17002461

A project dissertation submitted to the
Civil Engineering Programme
Universiti Teknologi PETRONAS
in partial fulfilment of the requirement for the
BACHELOR OF CIVIL ENGINEERING WITH HONOURS

Approved by,

AP Dr. Muhammad Raza Ul Mustafa

UNIVERSITI TEKNOLOGI PETRONAS
SERI ISKANDAR, PERAK
January 2022

CERTIFICATION OF ORIGINALITY

This is to certify that I am responsible for the work submitted in this project, that the original work is my own except as specified in the references and acknowledgements, and that the original work contained herein have not been undertaken or done by unspecified sources or persons.

Nurul Balkhis Athirah Binti Kamaruzaman

ABSTRACT

Flood is one of the disastrous events that lead to economic and properties loss which frequently impact Perak, Malaysia. The landscapes of Perak have significantly changed throughout the year due to the population expansion and development. Considering the effect of land use changes is important to develop flood risks map for planning mitigation approaches. The objectives of this study were to identify flood causative factors using Geographic Information System (GIS), to predict land use changes using GIS and Artificial Neural Network (ANN), and to develop flood risk maps using GIS. Maximum Likelihood Classification in ArcGIS was implemented for monitoring land use changes, whereas Artificial Neural Network Cellular Automata (ANN-CA) modeling using Quantum Geographic Information Systems (QGIS) has been implemented to predict the future land use changes. This study examined the land use changes in Perak for the years 2001, 2011, and 2021. The study also delivers predictions of future changes for the years 2031, 2041, and 2051. Furthermore, Analytical Hierarchy Process (AHP) was applied in this study to compare the relative importance of flood causative factors based on pairwise matrix in which eight relevant factors have been selected namely, rainfall intensity, drainage density, topographic wetness index, slope, elevation, land use, normalized difference vegetation index and soil types. Then, this study extend to present spatial analysis for the estimation of flood risk areas. The weightage comparison gained in AHP was input in the ArcGIS by using Weighted Overlay method. The flood risk maps for the year 2001 – 2051 were prepared for Perak region. The findings from ANN-CA simulation demonstrated that urban areas will grew rapidly and have a significant rise by 4555.10 km^2 to 4980.42 km^2, for 2031 – 2051. However, in the simulated years, the area of dense forests will reduce from 15087.61 km^2 to 14795.43 km^2. Based on the flood risk maps generated by AHP-GIS, it reveals that the area which have high and very high flood risk level were identified in the south-west part of Perak particularly at Manjung, Perak Tengah and Hilir Perak. The findings of this study provide critical information that could aid in the development of upcoming sustainable planning and management, along with helping the authorities in making assessments to enhance environmental and ecological conditions.

ACKNOWLEDGEMENT

In the name of Allah, the Most Gracious, the Most Merciful. Praise to Him the Almighty that in His will and given strength, I am able to finish the dissertation for Final Year Project. Special thanks to my supervisor, AP Dr. Muhammad Raza Ul Mustafa, for the enlightening supervision and countless hours devoted in giving out his insightful knowledge and valuable assistance throughout the completion of this project. Furthermore, his unwavering support and guidance from start to finish has inspired me to complete the project magnificently.

I would also like to convey my full appreciations to Mr. Mohammed Feras Baig, a full-time Master of Science Degree Student in Civil Engineering at Universiti Teknologi PETRONAS, for his support and knowledge sharing regarding my project. His cooperation and guidance was very essential for my understanding of this project.

Furthermore, a million thanks to Universiti Teknologi PETRONAS and Civil Engineering Department for providing students with valuable skills and excellent theoretical as well as practical work throughout the study period.

Finally, I thanked my parents, Mr. Kamaruzaman Yaacob and Mrs. Rohayati Mat Salleh, family and friends for their support, motivation and constructive advice. Thank you and may Allah bless all of you.

Thank you.

TABLE OF CONTENT

LIST OF FIGURES

LIST OF TABLES

SYMBOLS AND ABBREVIATIONS

GIS	Geographic Information System
QGIS	Quantum Geographic Information System
ANN-CA	Artificial Neural Networks – Cellular Automata
AHP	Analytical Hierarchy Process
DEM	Digital Elevation Model
NDVI	Normalized Difference Vegetation Index
TWI	Topography Wetness Index
USGS	United States Geological Survey
POWER	Prediction of Worldwide Energy Resource
DIVA	Data-Interpolating Variational Analysis
FAO	Food and Agriculture Organization
MCA	Multi-Criteria Analysis
IDW	Inverse Distance Weighting

CHAPTER 1

INTRODUCTION

1.1 OVERVIEW

The chapter herein discuss about the introduction of this project which includes background of study, problem statement, objectives and scope of study. It begins with a summary of the flood events as the background of study and goes ahead to summarize the relationship between the land use changes and flood risks within the study area of Perak, Malaysia. This study is concerned with the development of future land use changes and flood risk maps using Artificial Neural Network-Cellular Automata (ANN-CA) model and Geographic Information System (GIS) integrated with Analytical Hierarchy Process (AHP).

1.2 BACKGROUND OF STUDY

Floods are the most common type of natural disaster in the world and happen when an overflow of water inundates land that is normally dry. According to World Health Organization (n.d.), floods have affected more than 2 billion people worldwide for the period between year 1998 – 2017. It is also estimated that 75% of drowning deaths are due to flood disasters. The frequency of flooding issues that many relate it with climate change has risen particularly in the last few decades especially in Asia and Pacific countries (Asian Development Bank, 2013). Concurrently, sharply increasing number of populations in these developing countries have resulted to millions of people moving to marginal lands along low-lying coasts and flood-risk areas in cities (Asian Development Bank, 2013). Asa result, floods have caused extreme harm to both lives and properties.

Flood is not a new occasion, and it is the primary hazard affecting Malaysia. According to Department of Irrigation and Drainage (2019), the flood prone area in Malaysia are approximately 10.1% (33,298km^2) of the land area of the country, 5.7 million people are affected due to floods and the average annual flood damage is estimated RM1.15 billion. In the annual flood report by Department of Irrigation and Drainage (2019), all states in Malaysia experienced floods throughout 2019. The information regarding to flood events in all states of Malaysia have been tabulated as in Table 1.1.

TABLE 1.1. Information of Flood Events All Over Malaysia for Year 2019 (DID, 2019)

State	**Number of flood incidents by district**	**Maximum average daily rainfall (mm)**	**Maximum period of flood events (day)**	**Total evacuation of flood victims (people)**	**Estimated losses (RM)**	**Maximum flood depth (m)**
Perlis	7	91	1	146	-	0.6
Kedah	53	82	1	1,114	2,840,000.00	1.5
Pulau Pinang	31	111	1	388	-	2.9
Perak	65	91	1	2,279	-	1.2
Kelantan	18	82	7	18,683	18,290,400.00	2.0
Terengganu	9	180	8	11,384	2,305,000.00	3.0
Pahang	28	119	1	904	-	1.1
Selangor	93	85	1	537	-	1.0
Melaka	12	124	1	1,131	-	0.9
Negeri Sembilan	16	90	1.5	50	3,145,000.00	1.2
Johor	30	152	3	3,562	-	1.5
Sabah	39	143	8	7,443	5,000.00	2.8
Sarawak	118	117	20	1,328	-	3.7
WP Kuala Lumpur	10	99	1	212	-	0.9
WP Labuan	6	122	1	0	-	1.5
Total	**535**			**49,161**	**26,585,400.00**	

Many reports have been filed in Malaysia due to flooding since 1920s. Large floods usually occur in the Northern states of Malaysia causes by prolonged rainfall, especially in the convening months of November and December which severely impacted the state of Perak. In fact, during the latest 2019 floods in Perak, the flood occurred due to continuous heavy rainfall exceeding 80 mm in 1-2 hours in a day as well as the problem of the river blocking the flow of water (DID, 2019). In 2019, there have been a total of 65 flood events throughout the state of Perak as shown in Table 1.2.

TABLE 1.2. Frequency of Floods by District in Perak in 2019 (DID, 2019).

District	**Frequency of Flood**
Kuala Kangsar	7
Hulu Perak	3
Perak Tengah	8
Kerian	1
Manjung	1
Taiping	6
Kinta	13
Kampar	3
Batang Padang	9
Hilir Perak	14
TOTAL	**65**

Other than that, land use increase significantly with the number of populations in Perak. The land use changes have a significant effect on the flood risk especially in the area of urbanization, deforestation and cultivation. Hence, rapid development such as uncontrolled residential buildings and expansion of agricultural lands should be supervised to prevent any destructive effect in the future. The land use changes impact the climate systems which in turn affect the frequency and characteristics of the rainfall (Szwagrzyk et al., 2018). Thus, many relate the flood issues with the climate change (Asian Development Bank, 2013). Moreover, land use influence the formation of runoff from the rainfall events and affects the hydraulic flow of river channels which will cause the flood to happen in that area.

By implementing the flood management system with the adoption of many new technologies discovered nowadays, quick response or emergency alert can be provided. This will ensure the risk of fatalities are reduced and minimizing the property and environmental damages. Fortunately, advances in computer technology and the use of Landsat satellites have made it easier to track down land use changes and progress during the last several years. The application of remote sensing technology in combination with Geographic Information System (GIS) has revealed to be beneficial in discovering a variety of environmental features. In compared to other traditional procedures and surveys, remote sensing and GIS techniques have been found to recommend more precise and cost-effective data evaluation. Many models have been developed in recent years for the prediction of land use, such as Cellular Automata (CA), Markov models, Artificial Neural Network (ANN), binary logistic regression, and fractal models. In this study, the combination of ANN and CA was utilized to predict the future land use. The advantage of using this model is it could predict the multi-directional change and give better results compared to the non-combination model (Ullah et al., 2019)**.**

Since floods are inescapable, and in some flood-prone places, they may occur repeatedly. Many strategies have been used to lessen flood occurrences and their impact under these conditions. Flood forecasting, according to Asokan and Nakulraj (2020), is a method of evaluating and predicting the amount, timing, and duration of floods based on known features of a river basin. Due to its ability to manage spatial data, GIS is critical in the development of flood risk maps (Ogato et al., 2020).

Saaty's Analytical Hierarchy Process (AHP), which he established in the 1980s, is among the best potent Multi Criteria Analysis (MCA) methodologies in the field of flood risk management. The benefits of AHP include direct involvement in decision-making, the use of a comprehensive GIS and criteria evaluation uniformity (Luu et al., 2017). This study proposes the integrated AHP–GIS analysis comprised of eight causative factors in the flood risk assessment: rainfall, drainage density, topographic wetness index, soil types, elevation, slope, normalized differential vegetation index and land use. The satellite information will be used together with the AHP-GIS analysis.

1.3 PROBLEM STATEMENT

Flood events have been reported to be getting more frequent in recent years which has caused many people suffered catastrophic experience. In the year 2014, Perak has been hit by the worst flood events since 1967. According to Looi S. (2014), the number of flood victims in Perak that are forced to leave their homes are 7,587 victims from 1,031 families. It is undoubtedly shows that the flood leaves many negative impacts and damages to the society and their properties besides the economic losses.

Therefore, flood assessment method should be employed to predict flood risk areas and to control flood disaster in Perak. The advancement of technologies in current years have significantly contributes to the use of engineering in flood disaster management. Various methods have been discussed to develop and evaluate the flood model. It is important to utilize new ensemble modelsto improve the accuracy of flood risk maps and this can be done by using machine learning algorithms such as ANN. Many studies have employed the ANN-CA model to predict the future land use of a certain area. This model has significantly proven to yield a good prediction result. Recent study conducted by Zeshan, Mustafa and Baig (2021) have managed to predict the future land use of Perak up to year of 2050 by using the same model. However, the study does not correlate the land use prediction with the possibility of flood risk occurrence in that area.

Therefore, in this study, ANN-CA is used to predict the future land use of Perak for 2031, 2041 and 2051. Then, the prediction maps are further analyzed to generate the flood risk maps by using integrated AHP and GIS. Moreover, different flood causative factors such as elevation, slope, topographic wetness index, normalized differential vegetation index, rainfall intensity, drainage density and types of soil have been prepared for this study to compare the significance weightage in a pairwise matrix using AHP method. The AHP-GIS is implemented as spatial forecasting tools to map the flood risk areas in Perak according to their weights. Thus, this will increase the accuracy of generated flood risk map as other factors that contributes to flooding in Perak have also been considered.

1.4 OBJECTIVES

The main purpose of this study is to identify flood causative factors, to investigate the land use changes and to develop the flood risk map for Perak.

The specific objectives of the study are:

i. To identify the flood causative factors using Geographic Information System (GIS)
ii. To predict the land use changes using Geographic Information System (GIS) and Artificial Neural Network (ANN).
iii. To develop a flood risk map using the integrated Analytical Hierarchy Process (AHP) and Geographic Information System (GIS).

1.5 SCOPE OF STUDY

The objective of this study is to predict the land use changes using GIS and ANN, and to develop flood risk maps using GIS. This study investigate the land use changes for the years 2001, 2011, and 2021 by using Maximum Likelihood Classification in ArcGIS. The study also provides predictions of future land use changes for the years 2031, 2041, and 2051. The prediction was performed by applying ANN-CA modeling in QGIS. Furthermore, AHP was implemented in this study to compare the relative importance of flood causative factors based on pairwise matrix in which eight relevant factors have been selected namely, rainfall intensity, drainage density, topographic wetness index, slope, elevation, land use, normalized difference vegetation index and types of soil. Then, this study extend to present spatial analysis for the estimation of flood risk areas. The weightage comparison gained in AHP was input in the ArcGIS by using Weighted Overlay method. The flood risk maps for the year 2001 – 2051 were prepared for Perak region.

CHAPTER 2

LITERATURE REVIEW

2.1 OVERVIEW

This chapter discuss about the finding information which related to the scope of the project. The literature review was carried out to study the approach of similar studies done by other researchers in detecting flood risk areas in Malaysia as well as in other parts of the world. The initial focus of the study was to understand the basic fundamental knowledge available on flood, the approach and extent of achievements obtained from similar studies carried out by previous researchers. The literature review was focused on the following topics: flood, flood management, flood causative factors, land use changes Artificial Neural Network-Cellular Automata (ANN-CA), Geographic Information System (GIS) and Analytical Hierarchy Process (AHP).

2.2 FLOOD

2.2.1 Introduction

Flood is a common natural catastrophe that resulted to severe damages and harms. Severe floods have been on the rise around the world. Due to rapid economic progress, flood damage has become even more aggravated. In Malaysia, floods are the main natural hazards as the country is influenced by monsoon floods as well as flash floods and tidal floods (Chan, 2015). Adding to that, the study area, Perak state, has been reported to be hit by numerous of flood events. These occurrences have affected population, frequency, areal extent, and socio-economic damage (Kia et al., 2012). The flood situation in Perak during 2019 can be seen in Figure 2.1 and 2.2.

FIGURE 2.1 & 2.2. Flood situation in Perak (Malaysia Kini, 2019)

Flood-related damages have reached unprecedented levels due to a lack of preparedness in many parts of the world, including Malaysia, as well as the growing influence of climate change (Munawar et al., 2021). Flooding incidents have been on the rise around the world, necessitating the need to establish appropriate risk management strategies in the face of calamities (Zou et al., 2012). Flooding disasters have caused the loss of lives, crops, infrastructure, and economic resources (Zhang, Jindapetch & Buranapanichkit, 2019). According to Wang et al. (2013), the risks and losses related to floods are greater than those associated with any other climatic disaster. Flooding has become more common as a consequence of population growth and climate change (Yu et al., 2017). The development of settlements in coastal areas and river basins, which are certainly susceptible to flooding, has resulted from the expansion of commercial and residential sectors. Land use and essential infrastructure are also major aspects in determining the magnitude of floods and their propagation.

In many parts of the world, rising urbanization has resulted in flood plains among residential neighborhoods, increasing the flood dangers (Witherow et al., 2019). Several studies have been conducted to assess flood risks in a country or region. However, as technology advances, innovations in data-driven models and their contributions to flood risk management need more examination. Flood danger is currently mapped on a worldwide scale utilizing satellite imagery and remote sensing technology (Wedajo, 2017).

2.2.2 Flood Management

Flood management is a crucial process to guide the related locality and disaster agencies at all levels to formulate and employ their specific plans (Asian Development Bank, 2013). According to Munawar et al. (2021), the main practices implemented in flood management can be categorized as Flood Prediction, Flood Detection, Flood Mapping and Flood Hazard (Risk Assessment).

Currently, the focus of flood risk management systems is mostly on forecasting floods and producing maps to verify disaster-prone areas. There are two categories of flood management which many past analyses tend to emphasis on: pre or post disaster phases. Pre-flood studies generally focus on flood mitigation, planning, risk assessment, and hazard analysis, and post-disaster flood management studies are focusing on flood detection, mapping, damage assessment, and evacuation planning. (Munawar et al., 2021).

In addition, the constant growth of modern technology can help in managing real-time data which to be used for area of flood risk management. The strategy for both pre- and post-disaster flood management is based on image processing and machine learning. Machine learning algorithms were combined with data analysis in the pre-disaster phase to produce predictions about the likelihood of flood occurrences, their severity, and potential future loss. (Hernandez, 2014). Nevertheless, in the post-disaster phase, image processing have been used along with techniques based on machine learning to map inundated areas and make judgements associated to relief and rescue procedures (Arslan et al., 2017).

2.3 FLOOD CAUSATIVE FACTORS

Flood causative factors are related to numerous weather factors such as heavy rain, storm surges, and other factors like inadequate drainage systems and structural failures of dams (Zahari & Hashim, 2017). Understanding the flood causative factors and the interaction between them are crucial in developing the flood model (Kia et al., 2012). In past studies, various of flood causative factors have been utilized in developing the flood modelling such as elevation, soil types, land use, flow direction, flow accumulation, curvature, rainfall intensity,Topography Wetness Index (TWI), Normalized Differential Vegetation Index (NDVI) and historical flood density (Pradhan, 2009; Kia et al., 2012; Roslee, Tongkul, Mariappan& Simon, 2018; Khoirunisa, Ku & Liu, 2021).

However, the specific guideline has not been provided for selecting flood causative factors that affect flooding as it depends on the natural and physical properties of the study area (Ullah & Zhang, 2020). The chosen factors need to be the most applicable for flood risk assessment in the location of study location (Dang, Babel and Luong 2011). In determining the flood causative factors, a few steps need to be considered. According to Dang, Babel and Luong (2011), the criterion, its components, and indicators must define the nature of flood risk. Other than that, the data must be accessible and consistent for every component and should be easily understood to describe the complexness of the flood risk concept. Finally, the components should be quantifiable, recognizable, and measurable (Dang, Babel & Luong, 2011).

Common flood causative factors that have been used in past studies are rainfall intensity, drainage density, slope, land use and type of soil (Mandviwala, Joshi & Prakash, 2016; Cao et al., 2016; Dung et al., 2020; Ullah & Zhang, 2020). Furthermore, other factors have been chosen in the studies such as elevation, TWI, NDVI (Kia et al., 2012; Ullah & Zhang, 2020; Khoirunisa,Ku & Liu, 2021). These factors have a great influenced in conducting flood risk assessment for the reason that elevation affect the movement of the overflow direction and in the depth of the water level (Ogato et al., 2020), TWI is a physical interpretation of flood areas, which is an essential factor of a river catchment (Khoirunisa, Ku & Liu, 2021) and NDVI is a useful indicator in evaluating vegetation coverage and its effect on flooding in a basin (Ullah & Zhang, 2020).

2.4 LAND USE CHANGES

Change detection is the process of determining differences in any process by examining data over multiple time intervals (Singh, 2010). Over time, humans have made significant changes to the earth's surface. The effect of land use changes on hydrological activities has been brought to the attention of land use administrators and academics as a result of these considerable changes (Fei et al., 2018). Land use managers and decision makers can gain a better understanding of the interaction between human and natural activity by analyzing the pattern in change detection.

At the global scale, the vast growth in population is the most critical element in the transformation of land use (Lopez et al., 2001). The transformation of natural regions into industrial or agricultural fields is chiefly responsible for the significant variances in land cover, particularly in emerging countries (Jat, Garg & Khare, 2008). The loss of natural land, thick forests, and watersheds exerts significant strain on river basin hydrological regimes and mechanisms (Guerra, Puig & Chaume, 1998). It is critical to provide multi-temporal data sets for evaluating changes in land spatial features (Lu et al., 2004). The use of multi-temporal datasets simplifies the explanation of crucial land use changes and patterns (Roy & Inamdar, 2019). The introduction of Landsat satellites, as well as advances in computer technology, have made it easier to track changes and advancements over the last several decades. The combination of remote sensing technologies and a GIS has demonstrated to be efficient in recognizing a wide range of environmental variables. (Helmer, Brown & Cohen, 2000).

In order to examine land use changes, decision support systems are used (Matthews, 1999; De Kok et al., 2001, Fan et al., 2008; West and Turner, 2014; Yu et al., 2018). Decision support systems, which are evolving at a rapid pace, have permitted the active work of technology in management and planning. This study used an Artificial Neural Network (ANN) technique, which is one of the decision support systems. When the ANN technique (Atkinson and Tatnall, 1997; Hsu et al., 1997) is combined with GIS (Al-Kodmanyu, 2002; Prasannakumar et al., 2011), which is previously capable of creating highly powerful solutions, more stable and successful models can be generated (Olden et al., 2004).

Several models based on simulations have been created during the last two decades and are used to model land cover changes all around the world. This includes Markov chain analysis (MCA) or Markov models, Cellular Automata (CA), Cellular Automata–Markov models (CA–Markov), Artificial Neural Networks (ANN), Binary Logistic Regression, and Fractal models **(**Zeshan, Mustafa & Baig , 2021).

2.5 ARTIFICIAL NEURAL NETWORK (ANN)

2.5.1 Introduction

ANN is a computational model inspired and constructed to replicate biological nervous systems which are efficient to perform detailed information-processing activities such as data categorization and pattern recognition (Gopal, 2017). The function of an ANN is dictated by network structure and connection strengths, and it is composed of different simple processing nodes (Gopal, 2017). Same as biological neural networks, ANN can develop understanding by a learning process.

A wide variety of real-world problems can be addressed by using neural networks. According to Gopal (2017), neural networks are capable to be taught through experience to develop their performance and dynamically adjust to differences in the environment. Moreover, they are capable to handle the fuzzy or insufficient information and noisy data, and can be very useful, especially in conditions where it is not likely to specify the rules or steps that lead to the resolution of a problem. Consequently, they are fault tolerant. Furthermore, the ANN information-processing model is fundamentally parallel. Nowadays, ANNs are utilized in a range of specialties involving engineering, finance, artificial perception, and control and simulation (Gopal, 2017).

2.5.2 Artificial Neural Network – Cellular Automata (ANN-CA)

The use of ANN and CA together proposes a system that can predict multi-directional change and produce high-quality outcomes. The ANN-CA model, a nonlinear tool, has been effectively employed to simulate land use changes (Mahajan & Venkatachalam 2009; Pijanowski et al. 2014).

CA serves as a bottom-up simulation framework in the model. The transition rules of land use changes for CA are mined using ANN as data mining tools; this means that ANN is utilized to comprehend the underlying patterns in land use data (Yang, Chen & Zheng, 2016). By simulating the brain's ability to sort patterns through interconnected systems of numerous neurons, ANN has the benefit of being able to perceive interactions in data (Arekhi & Jafarzadeh 2014; Tayyebi & Pijanowski 2014). It is a good global parametric model for modelling land use changes, but different spatial drivers simulate land transformation in a non-linear way.

Furthermore, ANN is particularly useful at processing faulty and inferior data, as well as capturing non-linear, complex aspects in modelling procedures. As a result, it is widely believed that they are capable of producing improved modelling outcomes (Li & Yeh, 2002). Tayyebi et al. (2014b, 2014c) examined land transformation models based on ANN, classification, and regression tree, as well as the multivariate adaptive regression spline model, and found that ANN surpassed other models in both temporal and spatial accuracies**.**

2.6 GEOGRAPHIC INFORMATION SYSTEM (GIS)

All sorts of geographic and spatial data can be saved, retrieved, managed, presented, and evaluated with Geographic Information System (GIS). GIS data combines digital data with actual-world elements such as roads, land use, elevation, trees, and waterways. Discrete objects and continuous fields are two abstractions for real objects. For both types of concepts mapping references, raster images and vector images are utilized to save data in GIS. Mapped location attribute references are made up of points, lines, and polygons. Identifying point clouds, which integrate three-dimensional points with RGB information at each location to produce a 3D color image, is a new hybrid technique of storing data. Thematic maps created with GIS are more graphically descriptive of what they are trying to illustrate or establish.

GIS recognizes and analyses the spatial relationships that exist throughout digitally stored spatial data. GIS and remote sensing are trustworthy techniques that may be used to assess geo-environmental disasters by giving a cost-effective synoptic coverage of a large area. In recent years, advancements in GIS and remote sensing have been incorporated into the evaluation of environmental disasters, greatly facilitating flood risk mapping, flood risk assessment, and flood management (Arun & Premalatha, 2020).

The flood mapping application of GIS can be divided into three functions: information database, analytical tools, and decision support system (Kamarudin, 2020). As a result, the technique of multi-criteria evaluation is required for the GIS to integrate the criterion in order to build a more accurate flooding map, as GIS is capable of handling the geomorphological characteristics easily (Jain, Singh, & Seth, 2000). Not only that, but GIS tools can also categorize several levels of hazard, such as very high, high, moderate, low, and very low (Kourgialas & Karatzas, 2011). This demonstrates the effectiveness of using GIS for flood mapping.

2.7 ANALYTICAL HIERARCHY PROCESS (AHP)

In the 1980s, Analytical Hierarchy Process (AHP) was developed by Thomas Saaty to simplify and enhance the decision-making cycle. It is a statistical model which has the most effective methods of Multi-Criteria Analysis (MCA) in the area of flood risk management (Koem, 2020). Luu et al. (2017) stated that the direct involvement of decision-makers, the utilization of a complete geographic information system (GIS), and the consistency of criterion evaluation are all advantages of AHP. Certainly, AHP's use in analyzing diverse geo-hazards challenges, such as flood and landslide susceptibility, slope failure, groundwater vulnerability, and urban seismic vulnerability has been acknowledged by researchers, practitioners, and decision-makers (Dano et al., 2019).

In developing AHP for flood risk mapping, a pairwise comparison matrix will be used to rank various flood causative factors based on their impact level. The chosen methodological framework expresses the cumulative character of each criterion, making it useful for creating flood data at the local, regional, and national scales. However, AHP has two limitations: it relies on expertise and judgement, and it necessitates a large number of pairwise comparisons (Thanh and De Smedt, 2011). Furthermore, bias may emerge when the criterion and sub-criteria are related.

Hence, various studies were consulted in order to determine the primary flood evaluation criteria. For example, Sharir, Roslee and Mariappan (2019) considered eight parameters: rainfall, slope gradient, elevation, drainage density, land use, soil textures, slope curvatures and flow accumulation in their study to analyze the flood susceptibility at Kg. Kolopis area, Penampang, Sabah, Malaysia. Moreover, Elsheikh, Ouerghi and Elhag (2015) used four parameters including annual rainfall, basin slope, drainage network and the type of soil to map the flood risk in Terengganu, Malaysia. Whereas Sulaiman et al. (2015) has chosen six parameters: rainfall distribution, slope, distance from river, land use, drainage density and road density to conduct the flood hazard zoning and risk assessment for Bandar Segamat, Johor, Malaysia.

According to Saaty (1980), AHP represents an issue using hierarchical structures, and later develops priorities for solutions depending on the user's judgement which is based on paired comparisons. The importance of the evaluation criteria and their weights must be decided. There are six steps in the procedure (Saaty, 1980).

1. Analyzing a complex, unstructured situation into its constituent elements.
2. Formation of the AHP.
3. Matrix of paired comparisons based on imposed judgments.
4. Calculate the relative weights of each criterion by assigning values to subjective assessments.
5. Combine judgments to discover the most important variables.
6. Verify that assessments and judgements are consistent.

Calculating the consistency ratio is the most important aspects of AHP (Saaty 1980). The matrix in question can be judged acceptable if the consistency ratio is less than 0.1.

CHAPTER 3

METHODOLOGY

3.1 OVERVIEW

This chapter aim to discuss about the method and design used for this project, including all the materials used. It explains how the method of the study was carried out, and the data involved. This chapter also outlines the procedures, process and software that were used to prepare the data necessary to accomplish the objectives of this study.

3.2 STUDY AREA

The study area is located at Perak, North-West of Peninsular Malaysia which occupies an area of 21,035 km^2. Perak lies at longitude of 101.0901° E and latitude of 4.5921° N with an elevation of 42 m above sea level. This state has a tropical climate with the average annual temperature of 26.4 °C. The second-largest river basin in peninsular Malaysia which is Perak River basin, is situated inside the study area. Perak River that flows from Hulu Perak originates from the Titiwangsa Mountains to the Beting Beras Basah, Bagan Datoh has a river length of roughly 400 km. The total catchment area of Perak River is 14,908 km^2 which cover up about 70% of Perak state. The main tributaries in the surrounding area are Pelus River, Kinta River, Batang Padang River and Bidor River. As the study area is located at tropical climate, there is significant rainfall throughout the year. The recorded average annual rainfall at the Northeast part, particularly in the upper Temenggor Dam catchment is between 2400 mm to 3200 mm. The average annual rainfall increases between 2600 mm to 3400 mm at the Southeast part while the average annual rainfall of the whole study area is approximately 2300 mm.

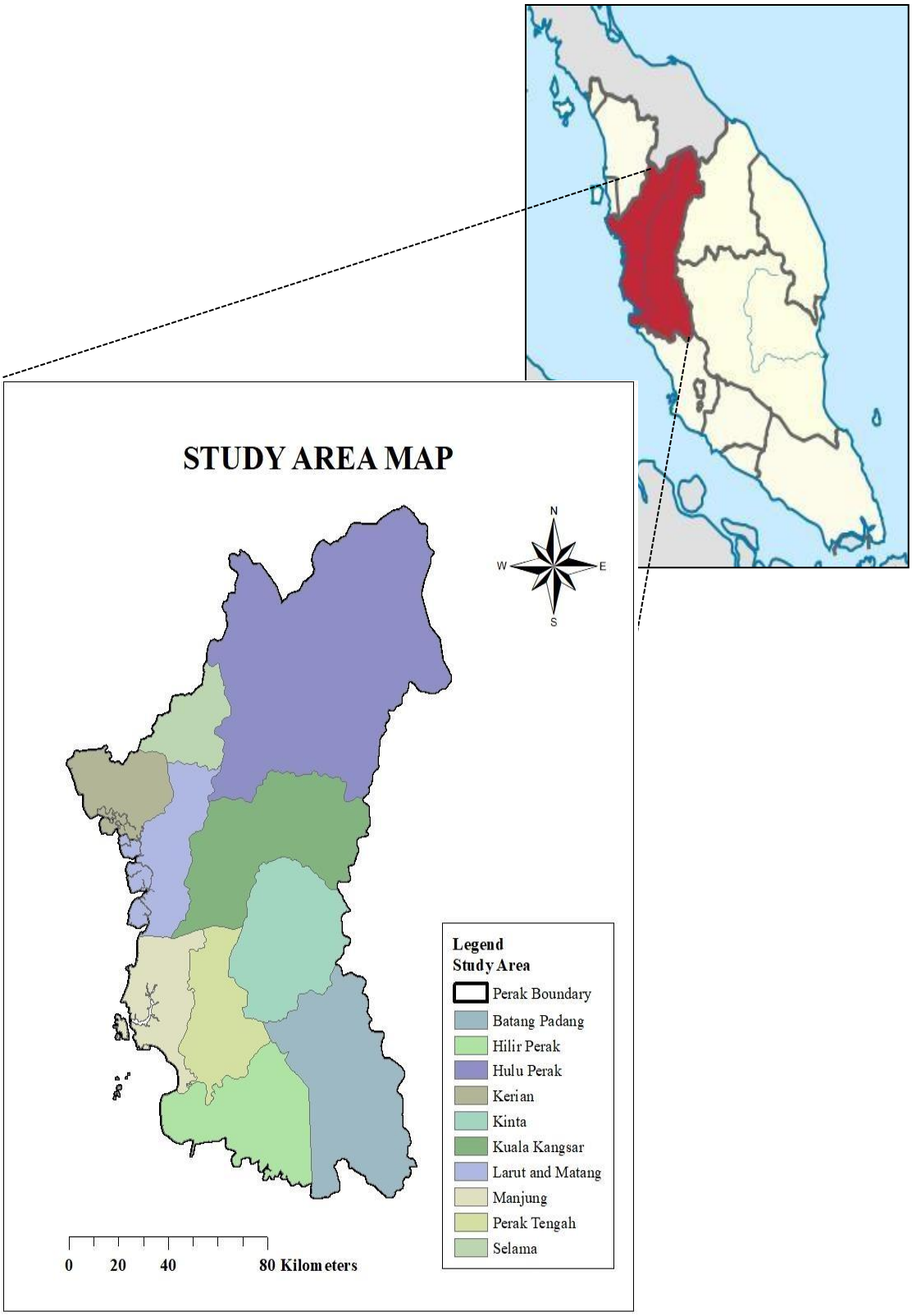

FIGURE 3.1. Study Area

3.3 PROJECT FLOWCHART

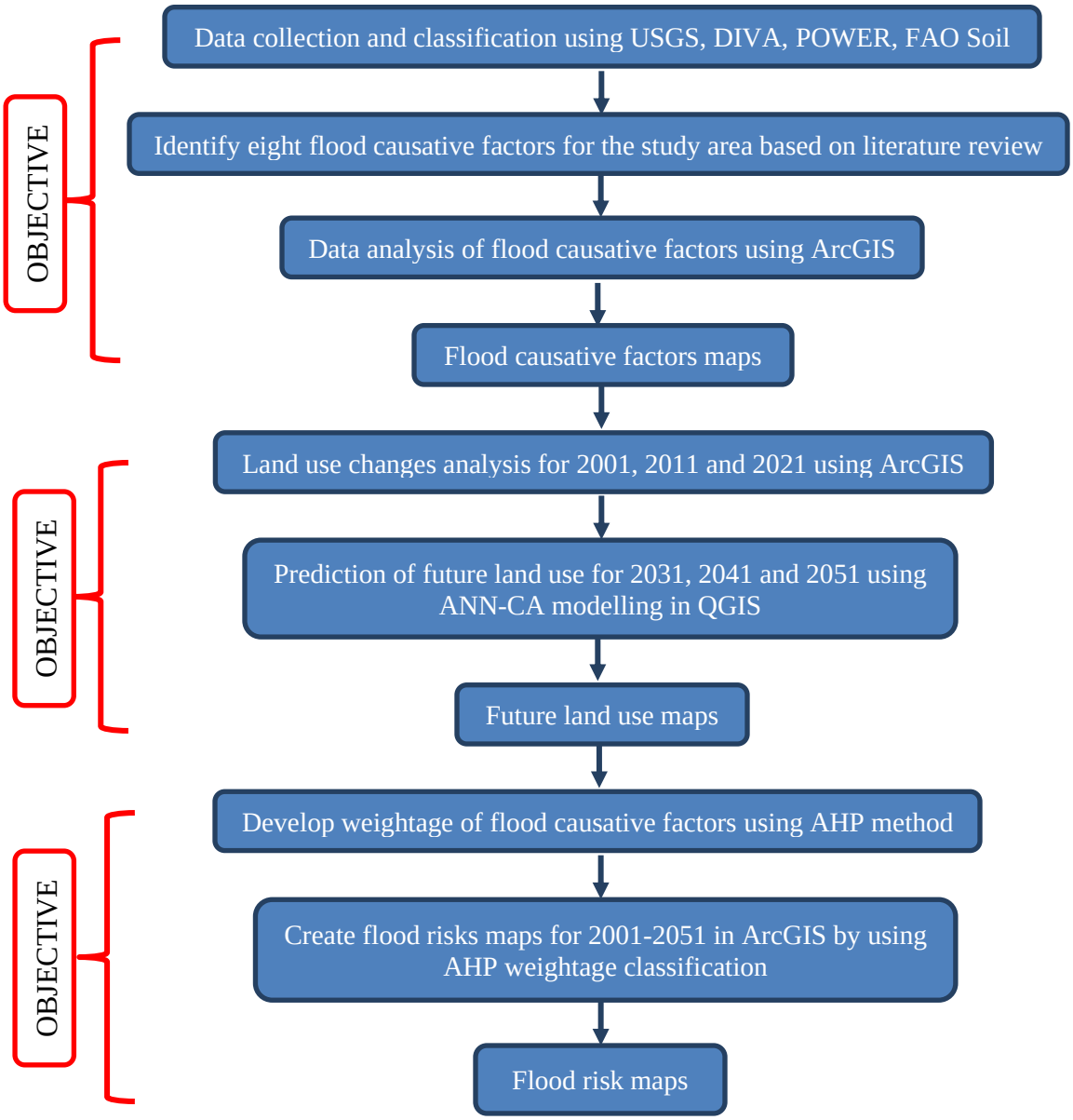

FIGURE 3.2. Project Flowchart

3.4 FLOOD CAUSATIVE FACTORS

Investigating the flood causative factors are the primary step in generating the flood risks map. These factors are determined by using the information obtained from the literature review. The selection of these factors are based on their interactions which is related to the flood history of Perak. There are eight flood causative factors that will be utilized in flood risk map which includes elevation, slope, TWI, soil types, land use, NDVI, rainfall intensity and drainage density.

3.5 PREPARATION OF DATA AND GEOSPATIAL LAYER

All data obtained in this study were added to ArcGIS to generate the flood causative factors maps. The ArcGIS 10.3 software package was employed for the analysis. All maps in this study were projected using the World Geodetic System 1984 Universal Transverse Mercator (WGS 1984 UTM) with the coordinate system of zone 47.

3.5.1 Study area

The shapefile of the study area was obtained from a website providing Data-Interpolating Variational Analysis (DIVA-GIS) from which the study area was clipped in ArcGIS.

3.5.2 Digital Elevation Model (DEM)

The United States Geological Survey (USGS) Earth Explorer website was used for acquiring the Digital Elevation Model (DEM) SRTM 1 Arc-Second Global. The data obtained in TIF format were divided into six images which covered the whole Perak. These images were layered together in ArcGIS to become a mosaic image. Then, it was extracted based on the boundary of Perak. DEMs are a valuable resource for determining topographic parameters that influence flood activity in a given area. Factors including slope, drainage density and TWI were extracted from the DEM, with a resolution of 30 m.

3.5.2.1 Slope

The slope analysis from spatial analyst tool (ArcToolbox in ArcGIS) was applied to generate the slope. The slope measurement was set to be in degree.

3.5.2.2 Drainage Density

Flow direction and flow accumulation raster dataset were prepared prior to creating a drainage density. These were done by applying hydrology analysis from spatial analyst tool. The flow direction will give information about the flow direction of water from the highest to the lowest elevation by each cell. While the flow accumulation represents the stream network by categorization of pixel values**.** Then, the drainage density was created by using line density from spatial analyst tool.

3.5.2.3 Topographic Wetness Index (TWI)

To produce TWI, flow accumulation and slope raster dataset were used by applying the Equation 3.1 as shown:

$$TWI = \ln \frac{\alpha}{\tan \beta + 0.01} \tag{3.1}$$

where α is flow accumulation and β is slope angle in degree. This equation was applied in raster calculator under spatial analyst tool.

3.5.3 Landsat Images

Four Landsat images were acquired from Landsat 8 OLI/TIRS Collection1 Level 1 for 2021 while Landsat 5 TM Collection 2 Level 2 for 2001 and 2011. The images were obtained from USGS Earth Explorer website, have a resolution of 30 m, was employed to generate the NDVI and land use maps.

3.5.3.1 Normalized Differential Vegetation Index (NDVI)

False color composites and indexes of vegetation were produced withnormalized differences. For improved visualization, the mixture of green, near-infrared (NIR), and red bands (R) was the false color composite that was utilized.NDVI were created for all images by using Equation 3.2:

$$NDVI = \frac{NIR - R}{NIR + R} \tag{3.2}$$

where NIR and R indicate the reflectance of the surface over nearly 0.8 μm and visible band (0.6 μm) in the spectrum of light, respectively (Zeshan, Mustafa and Baig, 2021). False color images helped in detection and visualization of different land characteristics, while NDVI was used to distinguish the vegetative in the study area. To create NDVI, this equation was applied in raster calculator under spatial analyst tool. For Landsat 8 image, Band 5 (NIR) and Band 4 (R) were applied while Band 4 (NIR) and Band 3 (R) were used for Landsat 5 images.

3.5.3.2 Land Use

The visible bands (red, green, and blue) were selected for land use classification. The bands selected for Landsat 5 classification were 3, 4, and 5, whereas 4, 5, and 6 bands were selected for Landsat8 image classification using Path/Row 127/56,127/57, 128/56 and 128/57 based on Perak state dataset. The images obtained from the satellite were sensed at various times of the year and all had the same spatial resolution of 30m as shown in Table 3.1. After verifying the Landsat scene by date, the subsequent four images were layered together before extracting it based on thestudy area.

To prepare the land use, image classification process was conducted by preparing training samples. This samples were chosen by identifying polygons across the delegate locations for each of the predetermined land use types. The study area has been classified into five classes which are forests, agriculture lands, urban areas, water bodies and barren lands.

After preparing the training samples, the signature file was created. The supervised classification technique has been used effectively in the case of spectral variability in individual types of cover, and hence it was utilized for the digital classification of Landsat images. In this study, the maximum-likelihood supervised classification method was applied.

TABLE 3.1. Detailed data for the Landsat images used for the study area

Year	Landsat scene ID	Path	Row	Date acquired
Landsat 5				
2001	LT51270562000237BKT00	127	56	24/08/2000
	LT51270572000077BKT00	127	57	17/03/2000
	LT51280562000020DKI00	128	56	20/01/2000
	LT51280571998062BKT00	128	57	03/03/1998
Landsat 5				
2011	LT51270562007144BKT00	127	56	24/05/2007
	LT51270572011187BKT00	127	57	06/07/2011
	LT51280562011098BKT01	128	56	08/04/2011
	LT51280572010047BKT00	128	57	16/02/2010
Landsat 8				
2021	LC81270562020068LGN00	127	56	08/03/2020
	LC81270572021038LGN00	127	57	07/02/2021
	LC81280562021045LGN00	128	56	14/02/2021
	LC81280572020059LGN00	128	57	28/02/2020

3.5.4 Soil data

The soil vector dataset was obtained from Food and Agriculture Organization, FAO-UNESCO Soil Map of the World website. The digital soil map of the world in ESRI shapefile format has been downloaded from the website and was added in ArcGIS. This data was clipped to the study area in. The soil types was categorized based on DOMSOIL classification under the symbology option.

3.5.5 Rainfall data

The list of rainfall stations in Perak were acquired from Department of Irrigation and Drainage (DID) while the average monthly rainfall data was generated from Prediction of Worldwide Energy Resource (POWER) from the year 2010 – 2020. There were 28 rainfall stations which has been identified in the study area with the details of it are shown in the Appendix A.

The average monthly rainfall data obtained was tabulated accordingly in Microsoft Excel similar to the table in Appendix A. This Excel file was then added to the ArcGIS. The rainfall intensity map was generated by using median rainfall through Inverse Distance Weighting (IDW) Interpolation in spatial analyst tool of ArcGIS.

3.6 LAND USE PREDICTION

ArcGIS was used for monitoring land use changes in Perak for the years 2001, 2011, and 2021. Then, Artificial Neural Network Cellular Automata (ANN-CA) modeling using Quantum Geographic Information Systems (QGIS) was implemented for the prediction of land use changes for the year 2031, 2041, and 2051.

3.6.1 Artificial Neural Networks Cellular Automata (ANN-CA) Modeling

ANN is considered as black-box method that tries to imitate the biological neural network. According to Kia et al. (2012), it is a mathematical model inspired by the structure and functions of human observation that can be instructed to perform a specific task using existing empirical data.

ANN algorithms are more accurate than other algorithms. Hence, it was used to train the transition potential model of land use. In recent decades, ANNs have become most common in remote sensing for proper land use modeling and classification. The most popular form of ANN is the multilayer perceptron (MLP). The MLP-ANN preprocesses the provided data from land use groups such as water bodies, forest, agricultural lands, urban areas and barren lands.

In this study, a combination of ANN and CA was managed to simulate and estimate the land use trends of Perak up to the year 2051 using open source QGIS software version 2.18.25. The CA feature in QGIS is based on the Markov chain algorithm. It relies on the present state of land use rather than the previous state. This model generates the output data in the form of tables and maps by combining previous and current land use maps with spatial input parameters. The spatial input parameters used in this study are elevation and slope. Based on that data, Modules for Land Use Change Simulations (MOLUSCE) plugin within QGIS software was used to train the model.

3.6.2 Transition Potential Modelling Using ANN

The transition potential modelling was trained using ANN with a momentum of 0.050, 1 pixel of neighborhood classification, hidden layers of 10 and a learning rate of 0.001 for the stabilization of learning graph. Furthermore, the number of iterations was set to 120 to prevent the issue of overfitting in the model. The land use transition matrix, which is an input for the ANN to obtain the transition probability, was created using changes in the area of different classes. Based on the transition potential model and geographical parameters, an ANN-CA simulation was used to simulate land use changes for 2021.

3.6.3 Validation of ANN-CA

Validation of model was conducted after the ANN-CA simulation, which allows for verifying, comparing, and validating the outcomes achieved. The method of validation was carried out by comparing simulated outcomes to the reference data which in this study, is the image classification for land use 2021.

Calibration and validation processes are critical factors in validating a simulation model. The kappa coefficient and percentage of correctness were used to statistically validate the simulation results. The predicted map of 2021 was obtained by inserting classified maps of 2011 and 2021 as input data. The predicted map of 2021 was matched with the image classification map of 2021 to assess the degree of agreement between the pixels of both maps. The overall kappa coefficient was calculated, the value of which ranges from 0 to 1. The high degree of agreement and satisfactory value of kappa coefficient indicated the validation of the simulation model. This validated simulation model formed the basis for future predicted maps of 2031, 2041, and 2051 by performing multiple iterations.

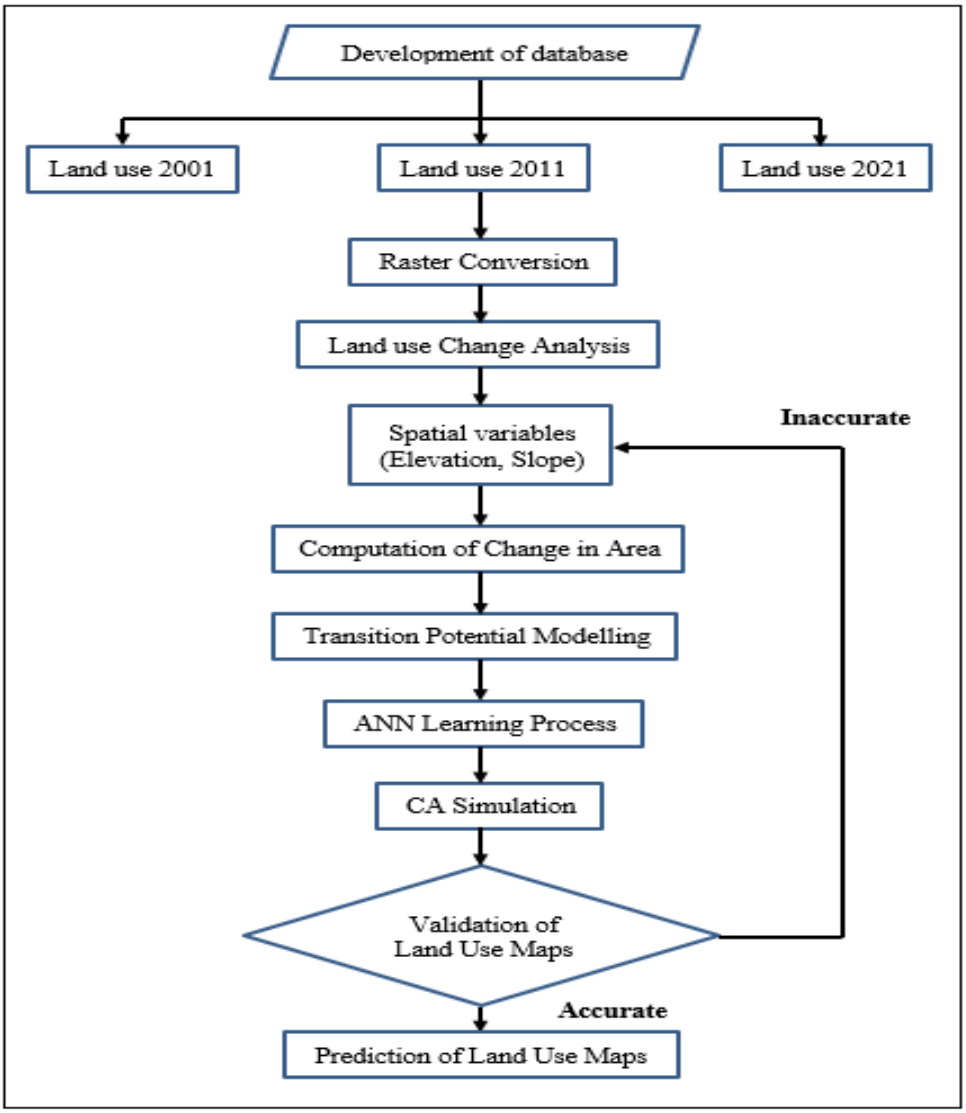

FIGURE 3.3. ANN-CA Flowchart

3.7 ANALYTICAL HIERARCHY PROCESS (AHP)

The selection of acceptable and sufficient criteria, as well as their standard processing and scale, determine the comprehensive hazard information (Dewan, 2013). Using Multi-Criteria Analysis (MCA), several research determined flood risk mapping (Bathrellos et al., 2016; Elkhrachy, 2015; Hoque et al., 2019). One of the most potent ways of MCA in the area of flood risk management is AHP, which was presented by Saaty in the 1980s. The advantages of AHP include direct involvement in decision-making, a full GIS combination, and criteria evaluation consistency (Luu et al., 2017).

The integrated AHP–GIS analysis, which comprises of three methodological approach was employed in this study. First, eight flood causative factors were determined: rainfall, drainage density, TWI, NDVI, land use, elevation, slope and soil types. The thematic layers of the factors were developed by using ArcGIS. The classification and sensitivity score of each factor was allocated based on recent studies.

Second, AHP was utilized to weigh all the causative factors. This was done by using Excel AHP template obtained from Goepel, K.D. (2012). The comparative value of flood causative factors have been evaluated in pairwise matrix to acquire the weighting coefficient from the eigenvectors of these factors during the process of AHP. Every factor has been allocated a value between 1-9, varying on its importance, (Saaty, 1980) which can be referred to Table 3.2.

TABLE 3.2. The definition of each intensity value assigned

Intensity	Definition	Explanation
1	Equal importance	Two elements contribute equally to the objective
3	Moderate importance	Experience and judgement slightly favor one element over another
5	Strong importance	Experience and judgement strongly favor one element over another
7	Very strong importance	One element is favored very strongly over another, its dominance is demonstrated in the practice
9	Extreme importance	The evidence favoring one element over another is of the highest possible order of affirmation
2, 4, 6, 8 can be used to express intermediate values		

Next, a consistency test was performed by verifying the consistency ratio (CR) in the pairwise comparison matrix. The ration of CR value was obtained by applying Equation 3.3 as shown:

$$CR = \frac{CI}{RI} \tag{3.3}$$

where CI is Consistency Index, RI is Random Inconsistency Index. The CI is expressed by using Equation 3.4:

$$CI = \frac{\lambda max - n}{n - 1} \tag{3.4}$$

where n is the number of parameters (flood causative factors) used. RI can be obtained as shown in Table 3.3 and it depends on the n value (Saaty, 1980). To ensure the matrix is consistent, the value of CR must be equal or less than 0.1 or 10%.

TABLE 3.3. RI value

Number of parameters (n)	2	3	4	5	6	7	8	9	10	11
Assigned RI	0	0.58	0.9	1.12	1.24	1.32	1.41	1.45	1.49	1.51

3.8 FLOOD RISK MAP

AHP was utilized as spatial forecasting tools to map the flood risk areas in Perak according to their significance weights. The thematic layer of each flood causative factors was mapped in raster format into the ArcGIS. Reclassification of every factor's category was done by using spatial analyst tool. The importance of the factors and their sub-categories was computed based on the Weighted Overlay Method with evaluation scale of 1 to 5 by 1. This method overlays several rasters using a common measurement scale and weights each according to its value. The input weightage of each factor was according to AHP result.

The flood risk map produced was categorized into five categories: very low, low, moderate, high and very high by using Jenks Natural Breaks Classification. Then, the area and its percentage for all categories were calculated to compare the changes of flood risk level throughout 2001 – 2051.

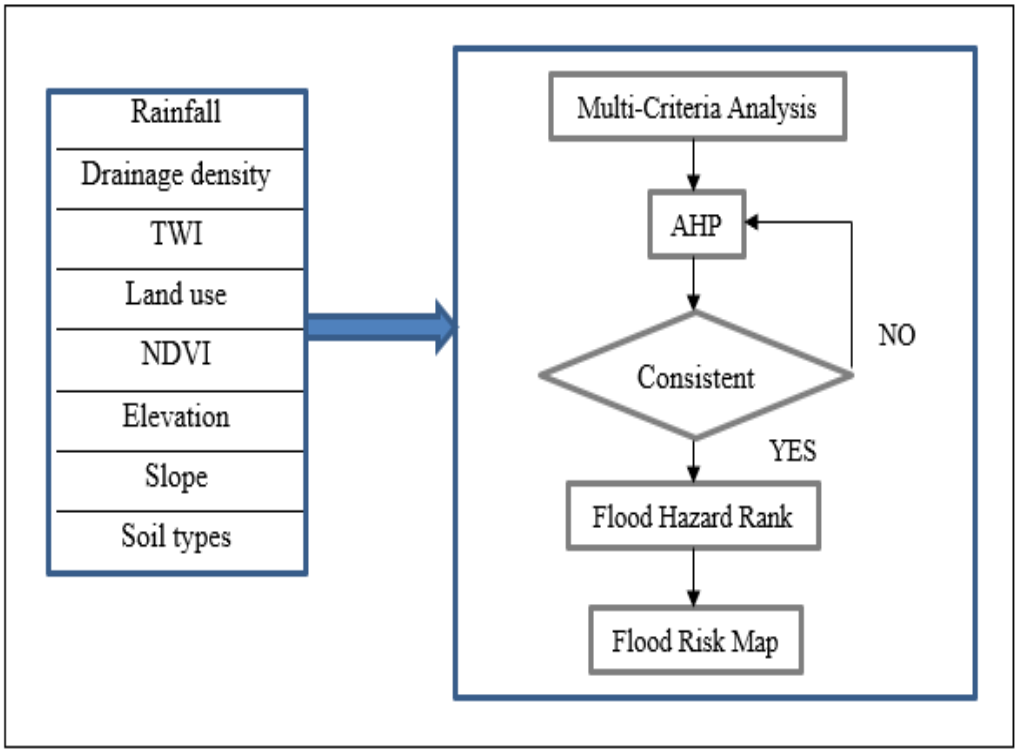

FIGURE 3.4. AHP Flowchart

CHAPTER 4

RESULTS AND DISCUSSION

4.1 OVERVIEW

This chapter is concerned with the data interpretations and presentations of results. All the results that have been developed throughout this study will be include in this chapter. It comprises of the discussion of every flood causative factors and their contribution to the flood issues. Furthermore, the chapter will further discuss about the analysis of land use prediction and flood risks maps that have been generated in this study. Analysis conducted was in accordance with the study aim and objectives.

4.2 FLOOD CAUSATIVE FACTORS

4.2.1 Elevation

Elevation plays a significant part in regulating the movement of the overflow pathand in the depth of the water level (Ogato et al., 2020). The elevation map is a visualization of altitude (Khoirunisa, Ku & Liu, 2021). According to Cao et al. (2016), the flow of water is from higher to lower elevation, and the flood risks will increase at the low elevation areas. Perak region is mostly made up of moderate, extended highlands with mild to steep slopes and elevations ranging from 27 to 2168 m above sea level (MSL). Figure 4.1 shows that the highest elevation rates above MSL are found in places to the North, such as Hulu Perak, Kuala Kangsar, Kinta, and Batang Padang. The steepness of slopes is directly related to the elevation of the study area, which has a direct relationship with soil erosion rate.

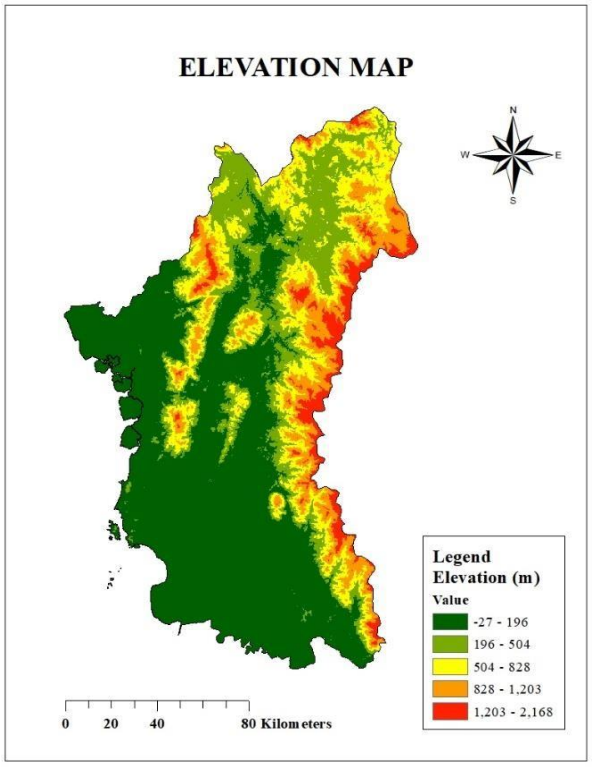

FIGURE 4.1. Elevation Map

4.2.2 Slope

Slope is a fundamental factor in flood studies as it regulates the surface water flow (Ullah & Zhang, 2020). Kia et al. (2012) defined that slope is the angle between the surface and horizontal datum which the velocity and runoff are induced by gravity. The relationship between slope and the surface velocity have positive correlation, and the surface runoff will increase significantly with higher magnitude of slope resulting to decrease of rainfall infiltration (Khoirunisa, Ku & Liu, 2021). Thus, the area with lower slope is prone to flood disaster situation as the water becomes stationary.

The steepness of Perak was estimated using a slope map. Five separate steepness classifications were generated from the slope map as indicated in Figure 4.2. The study area's topographical attributes were used to determine the steepness variation. The rate of soil erosion, soil stability, and sedimentation are all influenced by the slope steepness factor. The amount of soil erosion increases as the slope gradient increases due to a rise in surface runoff velocity.

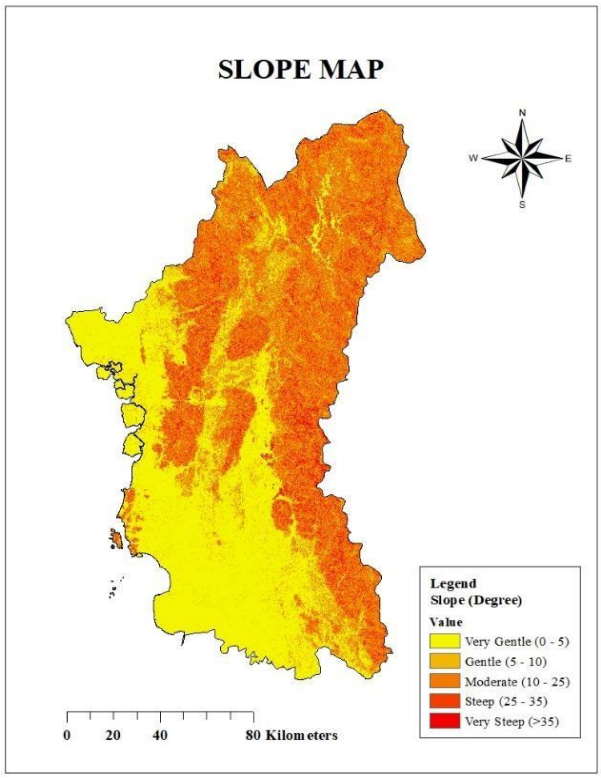

FIGURE 4.2. Slope Map

4.2.3 Drainage Density

Drainage density is described as the fraction of the overall span of the watershed channels to the entire region of the basin (Ullah & Zhang, 2020). This factor is affected by permeability, erodibility of surface materials, vegetation, slope and time (Ogato et al.,2020). Various reported floods happened due to accumulation of large quantity of water in low drainage density area. This factor is proven by a survey that have been conducted by Sahabat Alam Malaysia (2016) which found that the flood events that often hit some area at Perak was due to the drainage system in the area is not functioning well. As indicated in Figure 4.3, the drainage density of the study area is divided into five classes. High drainage density ratings favor runoff and, as a result, indicate a low flood risk. Flood risk will be reduced in basins with bigger drainage density values (Ajin.R.S. et al,2013).

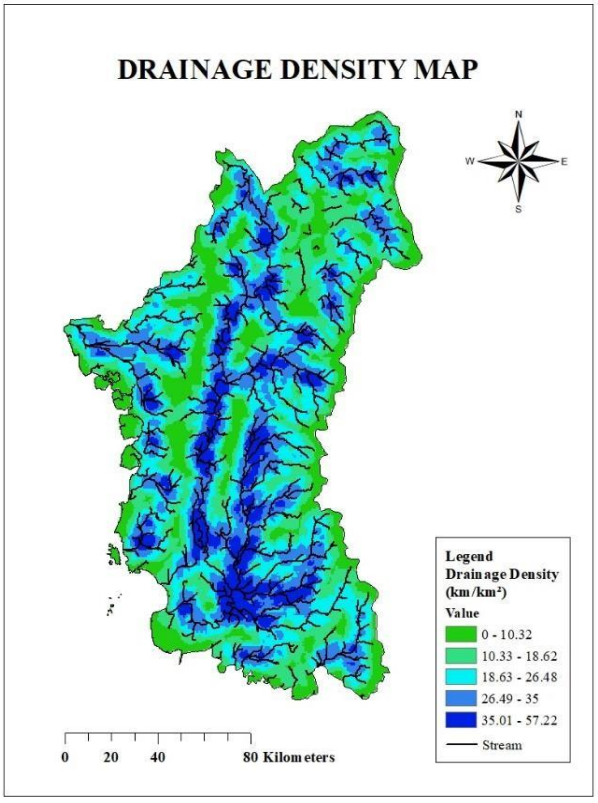

FIGURE 4.3. Drainage Density Map

4.2.4 TWI

The TWI is a natural interpretation of flood areas, which is a significant factor for the catchment of river. The TWI of a catchment implies two kinds of computations: flat lands and hydrographic positions. The TWI is usually utilized to evaluate topographic control of hydrological activities (Khoirunisa, Ku & Liu, 2021). The regions with high TWI have a high exposure to flooding while the regions with low TWI have lower flood risk (Ullah & Zhang, 2020).

In this study, TWI is another flood causative factor as it demonstrates the quantity of flow accumulation and the potential of the water to move downslope due to gravity. This factor is associated to soil moisture condition. The TWI map of the study area was created and ranged into five classes which are 2.11 – 5.58, 5.58 - 6.97, 6.97 – 8.75, 8.75 – 11.22 and 11.22 – 21.79 as shown in Figure 4.4.

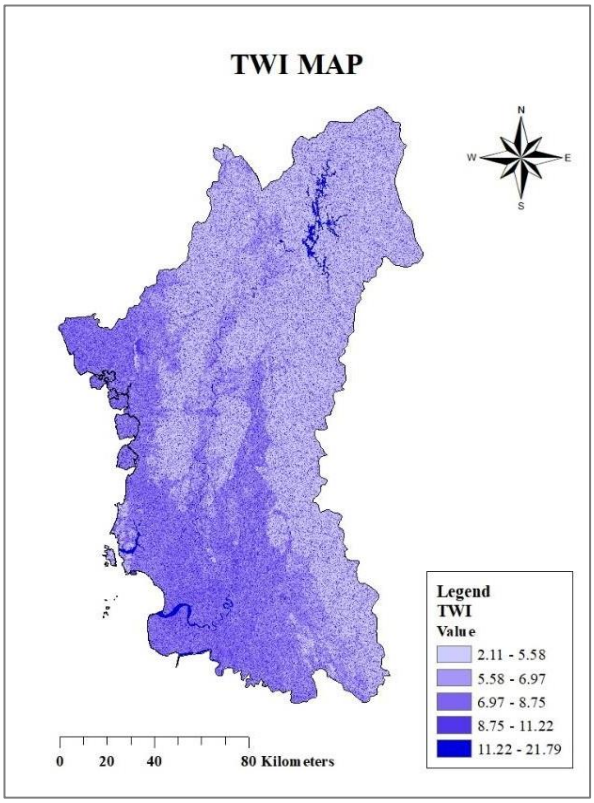

FIGURE 4.4. TWI Map

4.2.5 Rainfall

Extreme rainfall will result to floods. In Perak, flood occurrence usually happened after heavy rainfall. Ullah and Zhang (2020) point out that rainfall has a direct correlation with river flow and a significant amount of rainfall in a brief time can cause floods in semi-arid region.

The rainfall map was developed by using the rainfall data from 28 rainfall stations located in the study area. The rainfall distribution has a range of average monthly rainfall of 172 - 187 mm. From Figure 4.5, it can be observed that the north side area, Hulu Perak Kuala Kangsar, Kerian, Larut, Matang and Selama have the lowest rainfall distribution of 172 – 175 mm. The region at Perak Tengah has the highest rainfall distribution of 184 –187 mm per month.

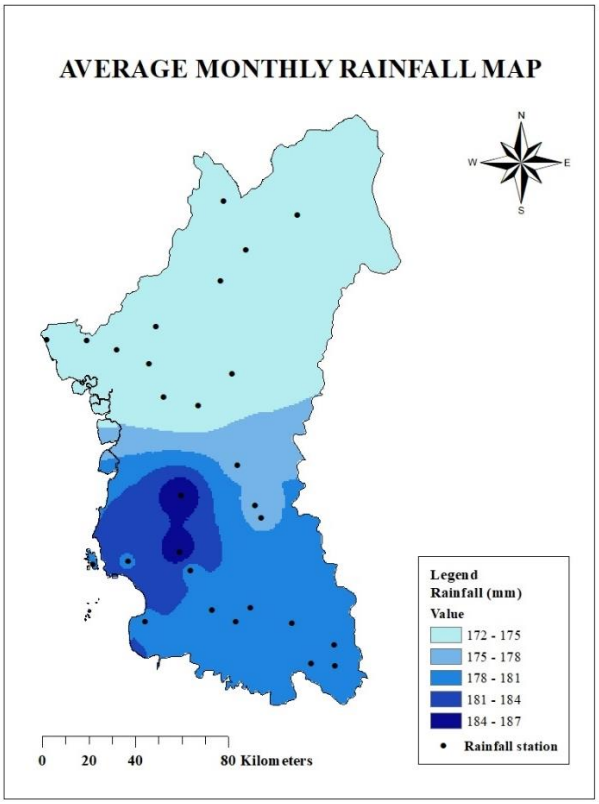

FIGURE 4.5. Average Monthly Rainfall Map for year 2010 – 2020

4.2.6 Soil types

The rainfall-runoff process is directly influenced by soil properties in a watershed, such as soil layer thickness, permeability, infiltration rate, and the degree of moisture in the soil prior to a rain event. (Zhiyu et al.,2013; Rimba et al., 2017). The composition and infiltration capability of soils will have a considerable impact on the soil's ability to absorb water. Different soils have different capacities. The likelihood of flooding increases when soil infiltration capacity decreases, resulting in increased surface runoff. When water is given at a rate that exceeds the soil's infiltration capacity, it runs down the slope as runoff and can create flooding on sloping area. (Ouma and Tateishi, 2014).

The classification of soil types for the study area are as shown in Table 4.1. The studyarea is described by seven types of soil series according to DOMSOI classification in ArcGIS. The spatial distribution of the soil types is shown in Figure 4.6. The most dominant type of soil is Orthic Acrisol which comprises of

71.21% and was discovered at the north until northeast of the study area. This followed by Eutric Gleysols (15.66%), Dystric Histosols (5.69%) and Ferric Acrisol (3.39%). These soil series were found in the northwest and south part of the region. Whereas small areas of Thionic Fluvisols (1.74%) and Eutric Fluvisols (0.004%) were found south and north part of the study area, respectively.

TABLE 4.1: Types of soil classification

No.	DOMSOI	Soil name	Area (km^2)	Percent (%)
1.	Ao	Orthic Acrisol	14724.40	71.21
2.	Ge	Eutric Gleysols	3238.51	15.66
3.	Od	Dystric Histosols	1176.67	5.69
4.	Af	Ferric Acrisol	701.89	3.39
5.	I	Lithosols	475.93	2.30
6.	Jt	Thionic Fluvisols	360.47	1.74
7.	Je	Eutric Fluvisols	0.76	0.004

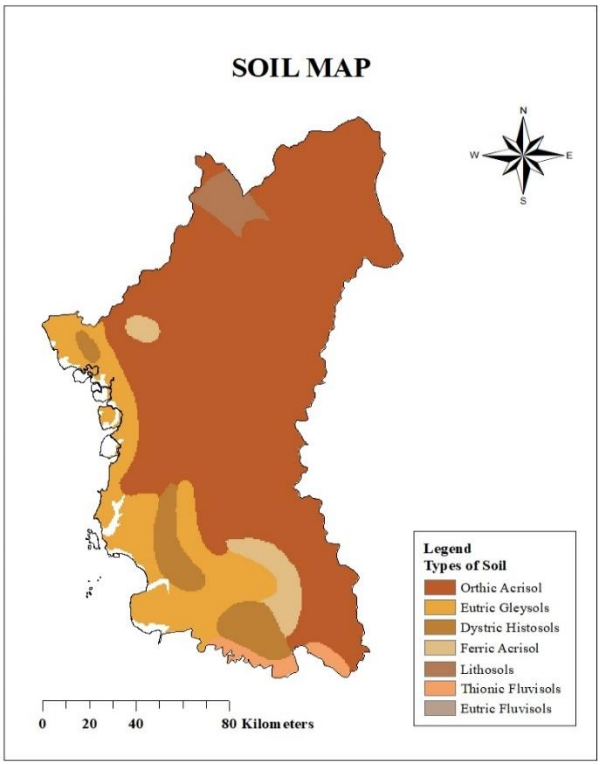

FIGURE 4.6. Soil Map

4.2.7 NDVI

NDVI is a frequently used vegetation index for analyzing worldwide vegetation coverage using satellite data. (Khoirunisa, Ku & Liu, 2021). It is a good tool for assessing vegetation cover and its impact on flooding in a basin. (Ullah & Zhang,2020).

The NDVI map of the study area was developed for the year 2001, 2011 and 2021. The maps were classified into five categories namely, water bodies, barren lands, grasslands, unhealthy vegetation and healthy vegetation (dense forest) as shown in the Figure 4.7 (a), (b) and (c). The categories were classified using a natural break method in ArcGIS. The NDVI value was generally in the range of -1 to +1. Negative values signify water, while positive ones reflect vegetation, hence NDVI has a negative association with flooding: higher NDVI values indicate a lower danger of flooding, while lower NDVI values indicate a higher risk of flooding (Khosravi et al., 2016).

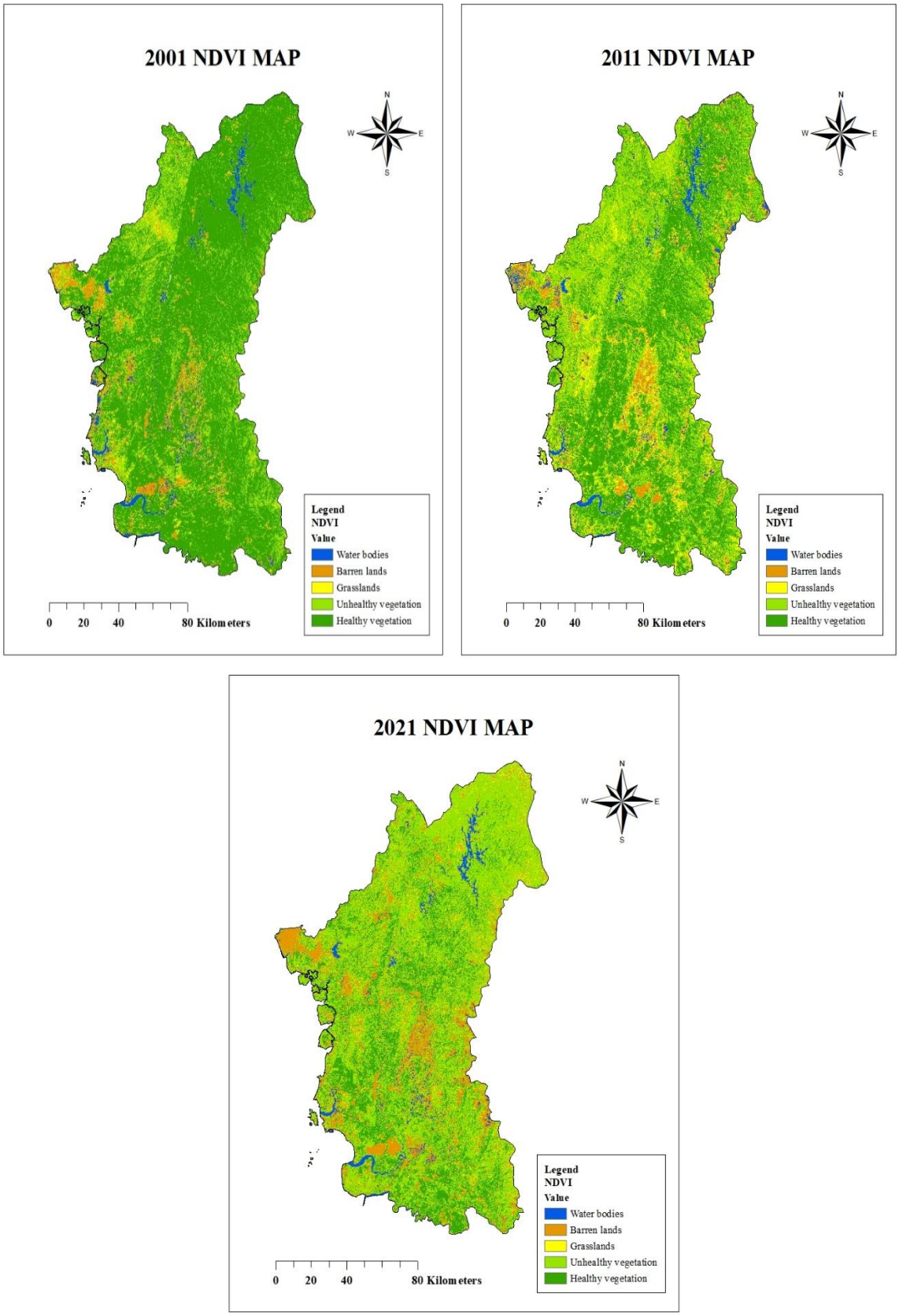

FIGURE 4.7. (a) 2001; (b) 2011; (c) 2021 NDVI Maps

4.2.8 Land Use Classification

According to Zeshan, Mustafa, and Baig (2021), the increase in barren and urban lands has resulted in a high danger of soil erosion in the watershed. Initially, the deep forests were turned to non-agricultural fields, and then to urban areas. Since flood occurrence is inversely proportional to vegetation density, some land use areas, in contrast to grassland areas, produce more storm runoff (Kia et al., 2012). By using Maximum Likelihood classification, the land use map of the study area for the year 2001, 2011 and 2021 were prepared as shown in the Figure 4.9 (a), (b) and (c). The maps were defined into five classes as descripted in Table 4.2.

TABLE 4.2. The classification scheme for land use

No.	Class	Description
1.	Waterbodies	Rivers, open water, lakes, ponds, and reservoirs.
2.	Forest	Natural forest, mangrove, and plantation forest.
3.	Agricultural lands	Mainly composed of grass, vegetation, crop plants, cultivated lands, and shrub lands.
4.	Urban areas	Residential and developed areas.
5.	Barren lands	Land areas of exposed soil

Calculating the area of each class and its percentage cover in the study area was used to examine changes in land use patterns of various classifications throughout time (Zeshan, Mustafa & Baig, 2021). The details of land use changes are given in the Table 4.3, Table 4.4 and Figure 4.8. In the year 2001, the major land cover in the study area was occupied by forests comprising 79.09% of the total area, followed by agricultural lands (10.27%), barren lands (5.24%), waterbodies (1.62%) and urban areas (2.05%). Compared to the year 2001, in 2011, the land cover experienced a decrease in forests (71.90%), followed by a considerable increase in barren lands (9.23%), urban areas (4.13%), agricultural lands(12.43%) as well as a slight decrease in the area of waterbodies (2.31%). However, for the year 2021, the observed land use changes were dominated by a sizeable increase in the urban areas (20.67%), a slight increase in forests (72.20%), followed by a decrease in barren lands (2.85%), agricultural lands (2.31%) and waterbodies (1.97%).

TABLE 4.3. The area of each class and its percentage for 2001, 2011 & 2021

Year	*2001*		*2011*		*2021*	
Land Use (Area)	**Area (km^2)**	**Percent (%)**	**Area (km^2)**	**Percent (%)**	**Area (km^2)**	**Percent (%)**
Forest	16568.13	79.09	15063.78	71.90	15126.53	72.20
Agriculture	2152.10	10.27	2605.38	12.43	483.34	2.31
Water bodies	700.87	3.35	484.96	2.31	412.37	1.97
Urban area	430.46	2.05	865.13	4.13	4329.45	20.67
Barren land	1097.97	5.24	1932.98	9.23	597.84	2.85

TABLE 4.4. Changes in area and percentage cover of land use classes for 2001 - 2021

Year	*2001 - 2011*		*2011 - 2021*	
Land Use (Area)	**Area (km^2)**	**Percent (%)**	**Area (km^2)**	**Percent (%)**
Forest	-1504.35	-7.19	62.76	0.31
Agriculture	453.27	2.16	-2122.04	-10.13
Water bodies	-215.92	-1.03	-72.58	-0.35
Urban area	434.66	2.07	3464.32	16.54
Barren land	835.01	3.98	-1335.14	-6.37

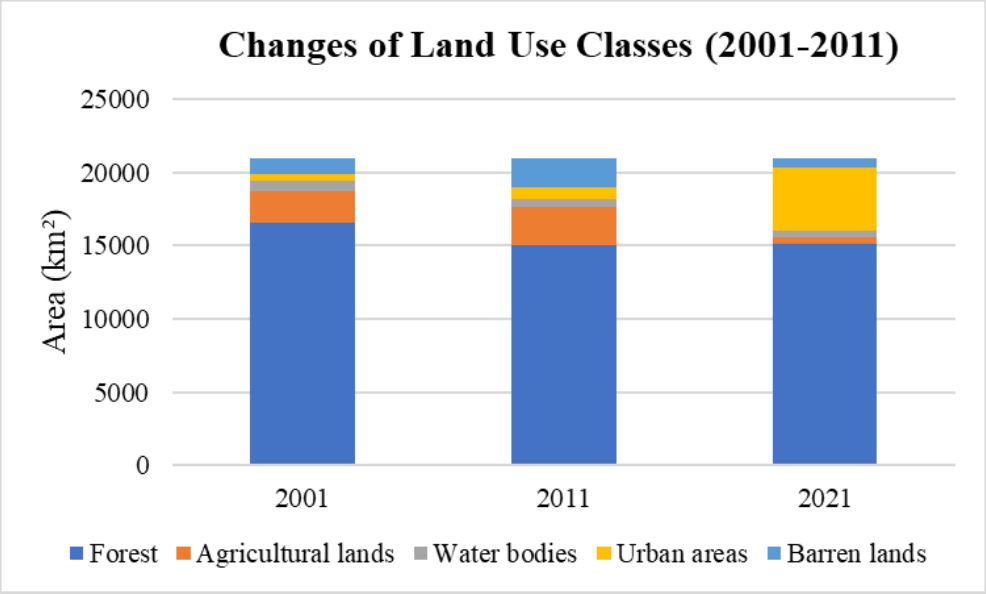

FIGURE 4.8. Land use change graph for 2001, 2011, and 2021

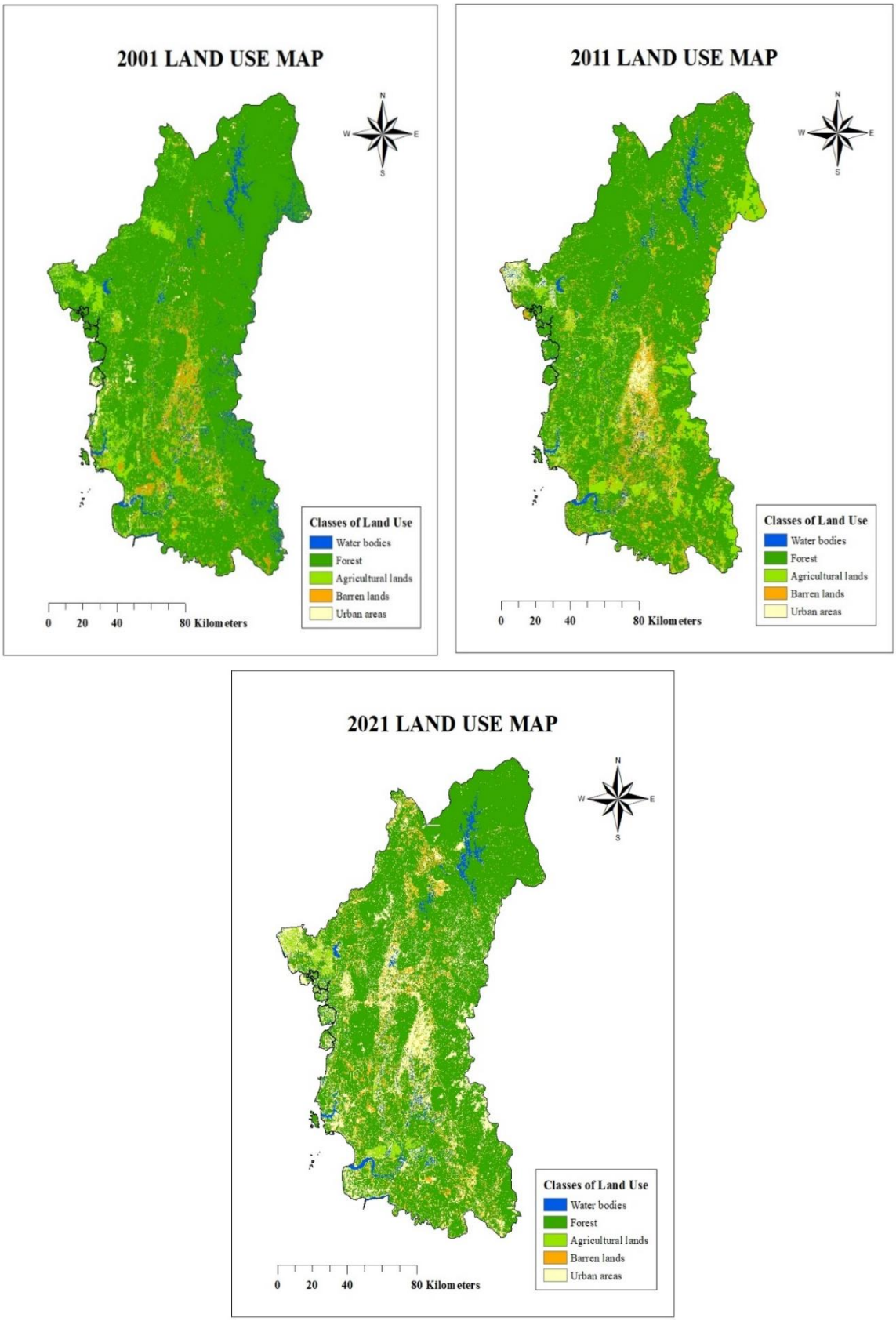

FIGURE 4.9. (a) 2001; (b) 2011; (c) 2021 Land Use Maps

4.3 PREDICTION OF LAND USE CHANGES

The spatial prediction of land use map for the year 2031, 2041 and 2051 are as shown in the Figure 4.11 (a), (b) and (c). The maps were defined into five classes as mentioned in Table 4.2.

The predicted maps of 2031, 2041, and 2051 were obtained by implementing multiple iterations of the validated simulation results of 2021. The percentage correctness of the simulation was 88.55% and the overall kappa coefficient, kappa histogram and kappa location were 0.75, 0.91 and 0.83, respectively. The percentage of correctness suggests that there would be 88.55% chance of correctness in predicted outcomes of 2031, 2041, and 2051 simulations when compared with the actual land use maps of 2031, 2041, and 2051. It also indicates that if the current land use changes would proceed in the same trend, then the future land use pattern for the Perak region would be comparable to the maps shown in Figure 4.11 (a), (b) and (c).

In the year 2031, the major land use in the study area are predicted to be occupied by forests comprising 72.02% of the total area, followed by urban areas (21.74%), barren lands (2.97%), waterbodies (1.76%) and agricultural lands (1.5%). Compared to the year 2031, in 2041, it is predicted that the land cover experienced an increase in urban areas and barren lands, 22.74% and 3.05%, respectively. The outcomes are followed by a slight decrease in forest (71.36%), water bodies (1.61%) and agricultural lands (1.23%). For the year 2051, the observed prediction of land use changes are the continuous increase in the urban areas (23.77 %) and barren lands (3.09%). The same trend is observed in 2051 as there are slight decrease in the area for forest (70.62%), waterbodies (1.49%) and agricultural lands (1.02 %), as shown in the Table 4.5 and Table 4.6. The increase in the land use changes for urban areas and barren lands might be due to the expected increase in commercial, residential, and industrial areas.

TABLE 4.5. The area of each class and its percentage for 2031, 2041 & 2051

Year	**2031**		**2041**		**2051**	
Land Use (Area)	**Area (km^2)**	**Percent (%)**	**Area (km^2)**	**Percent (%)**	**Area (km^2)**	**Percent (%)**
Forest	15087.61	72.02	14950.02	71.36	14795.43	70.62
Water bodies	369.57	1.76	337.92	1.61	311.44	1.49
Agriculture	314.50	1.50	257.79	1.23	213.95	1.02
Urban areas	4555.10	21.74	4764.91	22.74	4980.42	23.77
Barren lands	622.76	2.97	638.91	3.05	648.30	3.09

TABLE 4.6. Changes in area and percentage of land use classes for 2031 – 2051

Year	**2031 - 2041**		**2041 - 2051**	
Land Use (Area)	**Area (km^2)**	**Percent (%)**	**Area (km^2)**	**Percent (%)**
Forest	-137.59	-0.66	-154.58	-0.74
Water bodies	-31.64	-0.15	-26.48	-0.13
Agriculture	-56.72	-0.27	-43.84	-0.21
Urban areas	209.81	1.00	215.51	1.03
Barren lands	16.15	0.08	9.40	0.04

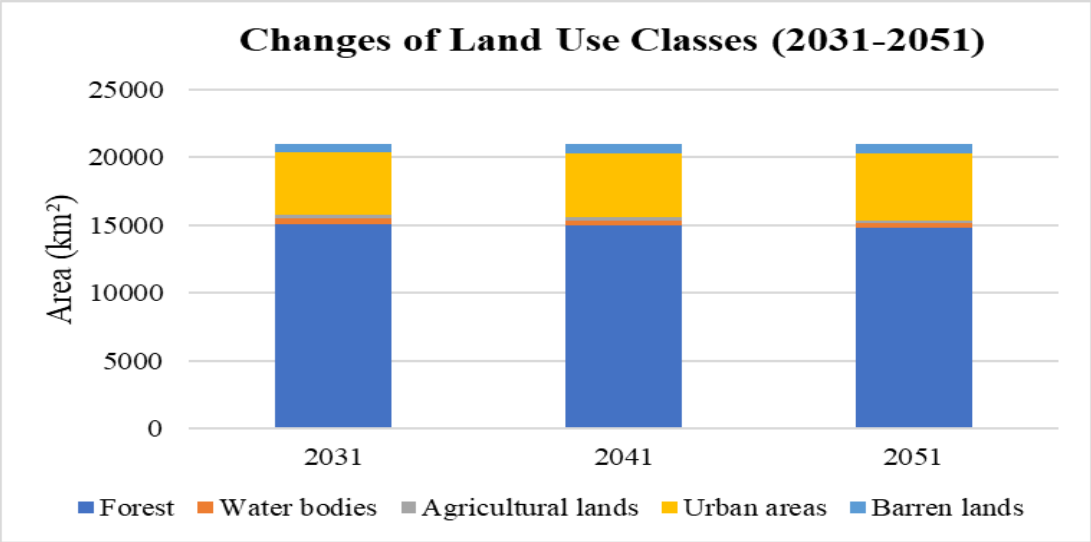

FIGURE 4.10. Land use change graph for 2031, 2041, and 2051

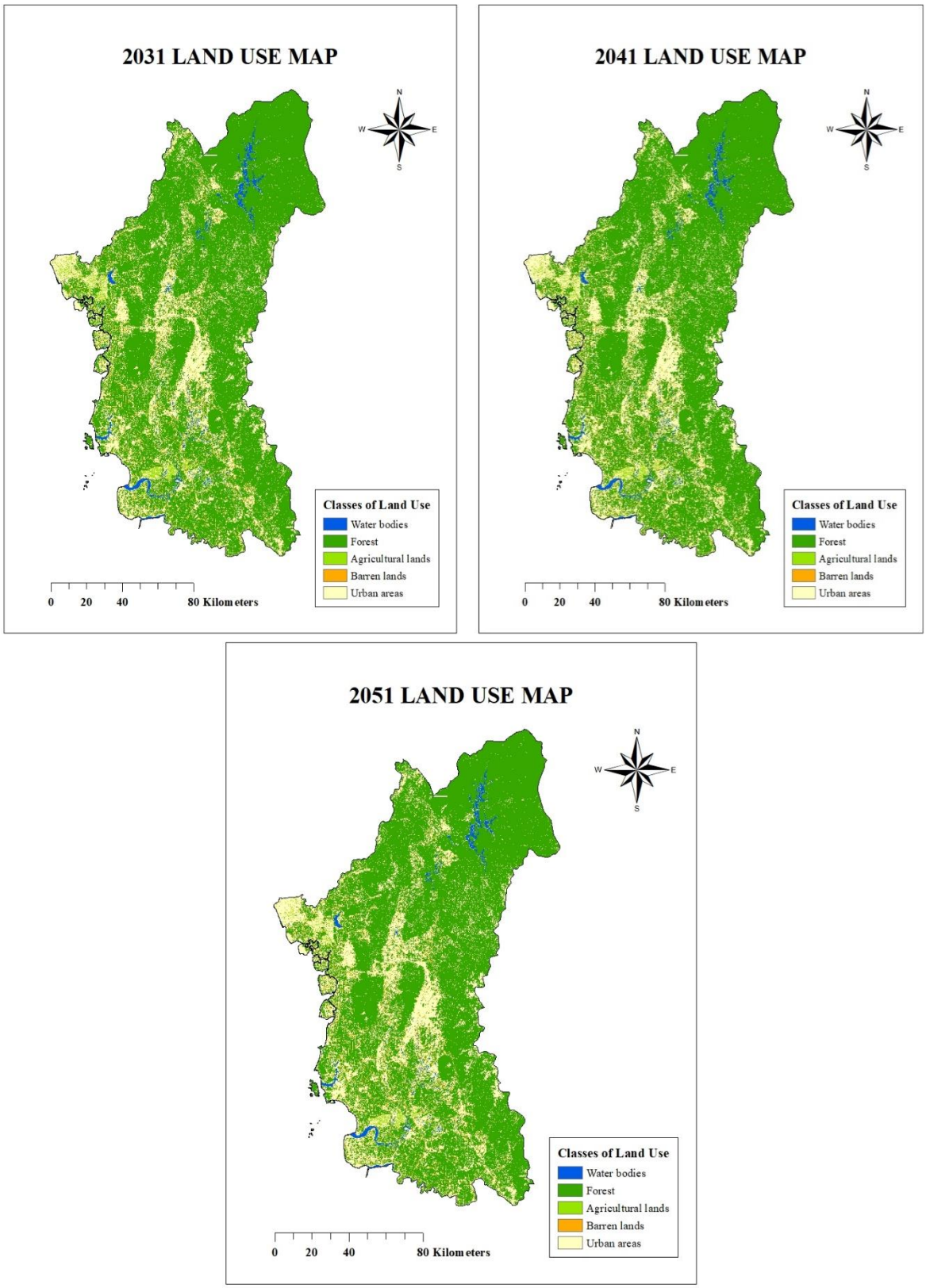

FIGURE 4.11. (a) 2031; (b) 2041; (c) 2051 Land Use Prediction Maps

4.4 FLOOD RISK MAP

The AHP analysis in this study includes eight flood causative factors in the assessment of flood risks across Perak: rainfall, drainage density, TWI, land use, NDVI, elevation, slope and soil types. An 8 x 8 pairwise matrix was created utilizing these factors to compare the relative significance and weight of each factor.

The significance level of each factor was rated using nine fundamental scale as shown in Table 3.2. Table 4.7 shows the pairwise comparison matrix developed for this study. The value of each row in the matrix define the importance between two factors. The relevance of rainfall in comparison to other characteristics is presented in the first row of the table. Rainfall, for example, is equally important to the drainage density, thus it is given a value of 1. The row contains the pairwise inverse values. As a result, the drainage density's worth is divided by one. Whereas Table 4.8 indicates the normalized pairwise comparison matrix. It is calculated by dividing all the column components by the sum of the column in the pairwise comparison matrix.

Rainfall (24.1%) and drainage density (24.1%) were defined as the most important factors to cause flooding in Perak as mentioned in the flood report by DID (2019). TWI (20.3%) was considered as second significant factor as flooded areas are mostly located at wet areas. Land use (10.6%) and NDVI (6.9%) were regard as strongly significant while elevation (5.0%) and slope (6.2%) were moderate significant. Finally, soil types (2.8%) is described as lower significant.

After generating pairwise comparison matrix, the relative relevance of each criterion was estimated using the AHP. The consistency check of the AHP analysis was conducted. CR value in this study is 0.035, which is less than 0.1. As a result, the pairwise comparison is both valid and consistent. Then, the flood risk map was developed after applying the weighting total of all causative criteria. The sensitivity score of each factor's sub-categories can be referred in the Appendix B. Table 4.9 indicates the weightage of each factor generated from AHP.

TABLE 4.7. Pairwise comparison matrix

Factor	***Rainfall***	***Drainage density***	***TWI***	***Land use***	***NDVI***	***Elevation***	***Slope***	***Soil***
Rainfall	1	1	1	3	4	5	5	6
Drainage density	1	1	1	3	4	5	5	6
TWI	1	1	1	2	3	4	4	5
Land use	1/3	1/3	1/2	1	1	3	3	4
NDVI	1/4	1/4	1/3	1	1	2	1/2	3
Elevation	1/5	1/5	1/4	1/3	1/2	1	1	3
Slope	1/5	1/5	1/4	1/3	2	1	1	3
Soil	1/6	1/6	1/5	1/4	1/3	1/3	1/3	1
Total	3.2	3.2	3.5	7.9	11.8	16.3	14.8	3.2

TABLE 4.8. Normalized pairwise comparison matrix

Factor	***R***	***DD***	***TWI***	***LU***	***NDVI***	***E***	***Sl***	***S***	**Weight**
Rainfall, R	0.32	0.32	0.28	0.38	0.34	0.31	0.34	0.24	0.241
Drainage density, DD	0.32	0.32	0.28	0.38	0.34	0.31	0.34	0.24	0.241
TWI	0.32	0.32	0.28	0.25	0.25	0.24	0.27	0.20	0.203
Land use, LU	0.11	0.11	0.14	0.13	0.08	0.18	0.20	0.16	0.106
NDVI	0.08	0.08	0.09	0.13	0.08	0.12	0.03	0.12	0.069
Elevation, E	0.06	0.06	0.07	0.04	0.04	0.06	0.07	0.12	0.050
Slope, Sl	0.06	0.06	0.07	0.04	0.17	0.06	0.07	0.12	0.062
Soil, S	0.05	0.05	0.06	0.03	0.03	0.02	0.02	0.04	0.028

TABLE 4.9. Weightage of each factor

No.	**Factors**	**Weights (%)**
1.	Rainfall	24.1
2.	Drainage density	24.1
3.	TWI	20.3
4.	Land use	10.6
5.	NDVI	6.9
6.	Elevation	5.0
7.	Slope	6.2
8.	Soil types	2.8

4.4.1 Flood Risk Maps for 2001, 2011 and 2021

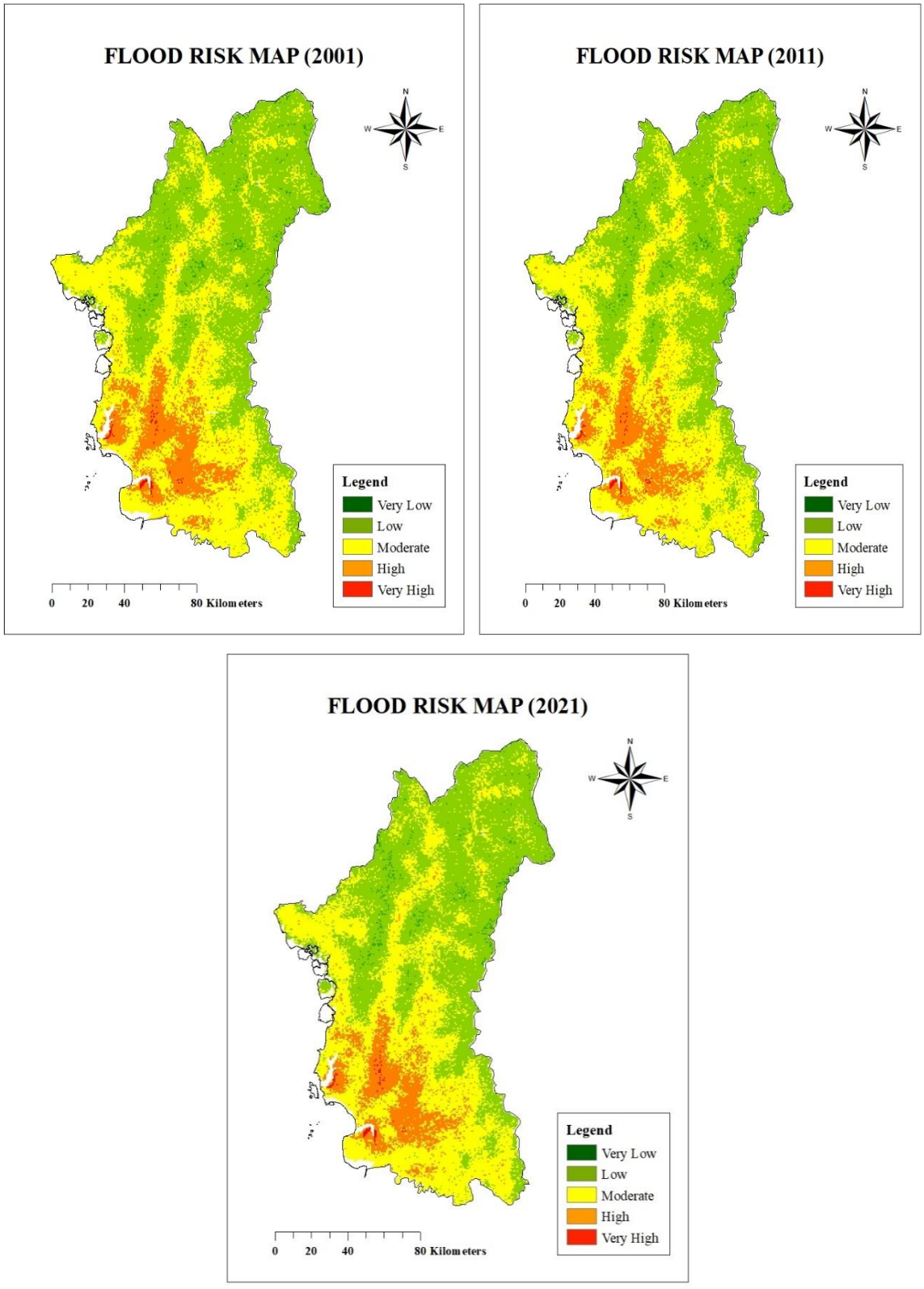

FIGURE 4.12. (a) 2001; (b) 2011; (c) 2021 Flood Risk Maps

TABLE 4.10. The area of each risk level and its percentage for 2001, 2011 & 2021

Year	**2001**		**2011**		**2021**	
Risk Level	**Area (km^2)**	**Percent (%)**	**Area (km^2)**	**Percent (%)**	**Area (km^2)**	**Percent (%)**
Very low	227.36	1.12	278.36	1.37	245.26	1.21
Low	9027.04	44.37	9183.31	45.12	9213.70	45.32
Moderate	8763.33	43.08	8783.95	43.16	8721.55	42.90
High	2277.38	11.19	2062.50	10.13	2101.57	10.34
Very high	48.84	0.24	43.41	0.21	47.75	0.23

TABLE 4.11. Changes in area and percentage of risk level for 2001 – 2021

Year	**2001 - 2011**		**2011 - 2021**	
Risk Level	**Area (km^2)**	**Percent (%)**	**Area (km^2)**	**Percent (%)**
Very low	51.01	0.25	-33.10	-0.16
Low	156.27	0.75	30.39	0.20
Moderate	20.62	0.09	-62.40	-0.26
High	-214.88	-1.06	39.07	0.20
Very high	-5.43	-0.03	4.34	0.02

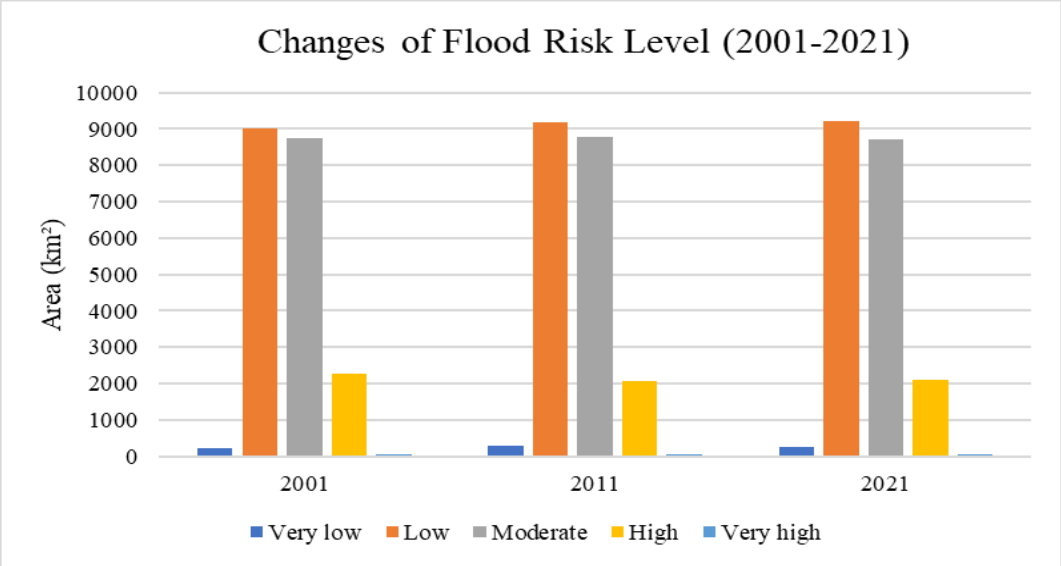

FIGURE 4.13. Changes of the flood risk level for 2001, 2011 and 2021

4.4.2 Flood Risk Map for 2031, 2041 and 2051

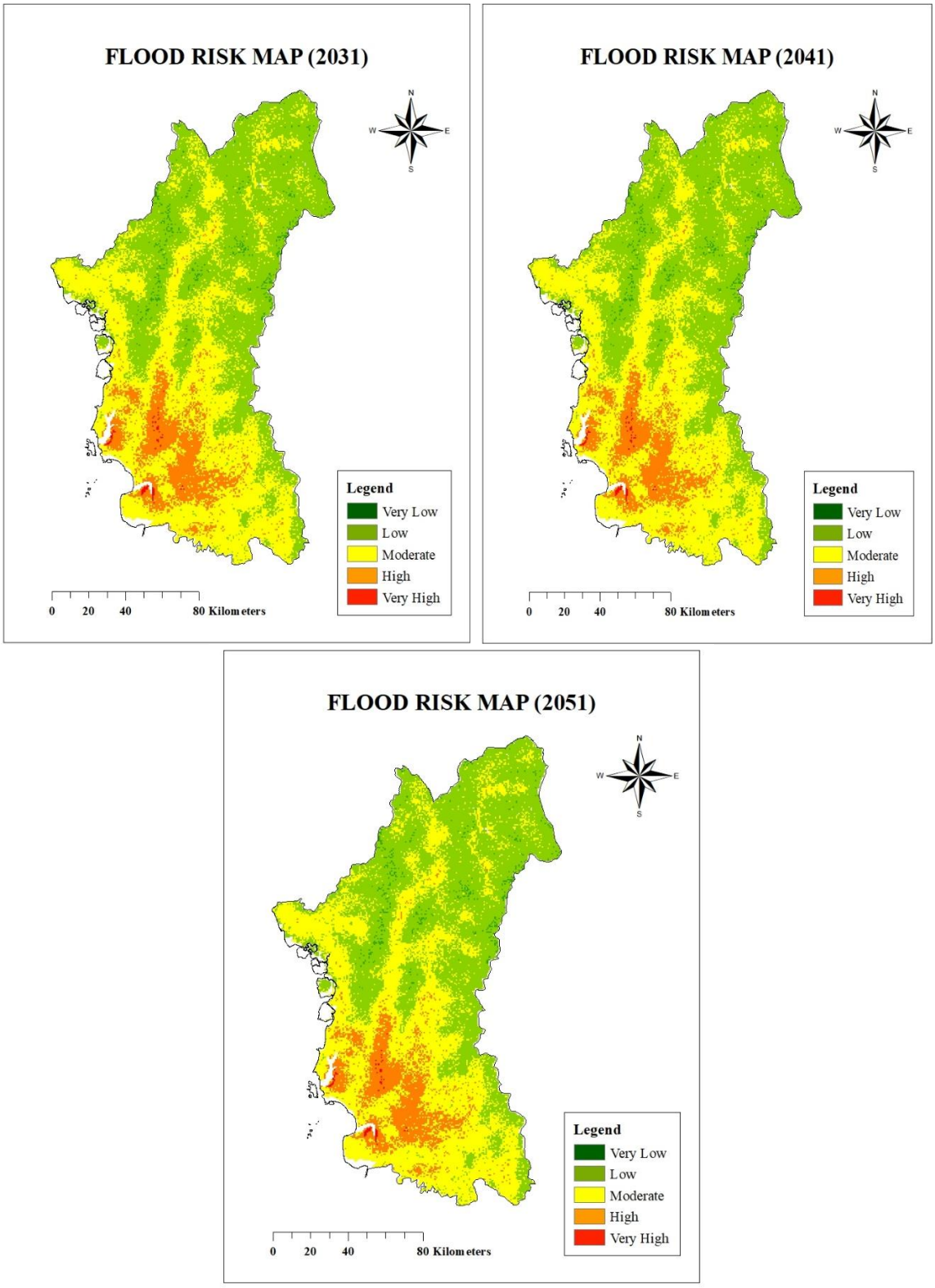

FIGURE 4.14. (a) 2031; (b) 2041; (c) 2051 Flood Risk Maps
TABLE 4.12. The area of each risk level and its percentage for 2031, 2041 & 2051

Year	2031		2041		2051	
Risk Level	Area (km²)	Percent (%)	Area (km²)	Percent (%)	Area (km²)	Percent (%)
Very low	238.75	1.17	237.67	1.17	237.67	1.17
Low	9220.22	45.35	9239.75	45.45	9244.63	45.47
Moderate	8751.39	43.05	8749.76	43.04	8755.73	43.07
High	2074.98	10.21	2057.62	10.12	2050.02	10.08
Very high	44.49	0.22	45.04	0.22	41.78	0.21

TABLE 4.13. Changes in area and percentage of risk level for 2031 – 2051

Year	2031 - 2041		2041 - 2051	
Risk Level	Area (km²)	Percent (%)	Area (km²)	Percent (%)
Very low	-1.09	-0.01	0.00	0.00
Low	19.53	0.10	4.88	0.02
Moderate	-1.63	-0.01	5.97	0.03
High	-17.36	-0.09	-7.60	-0.04
Very high	0.54	0.00	-3.26	-0.02

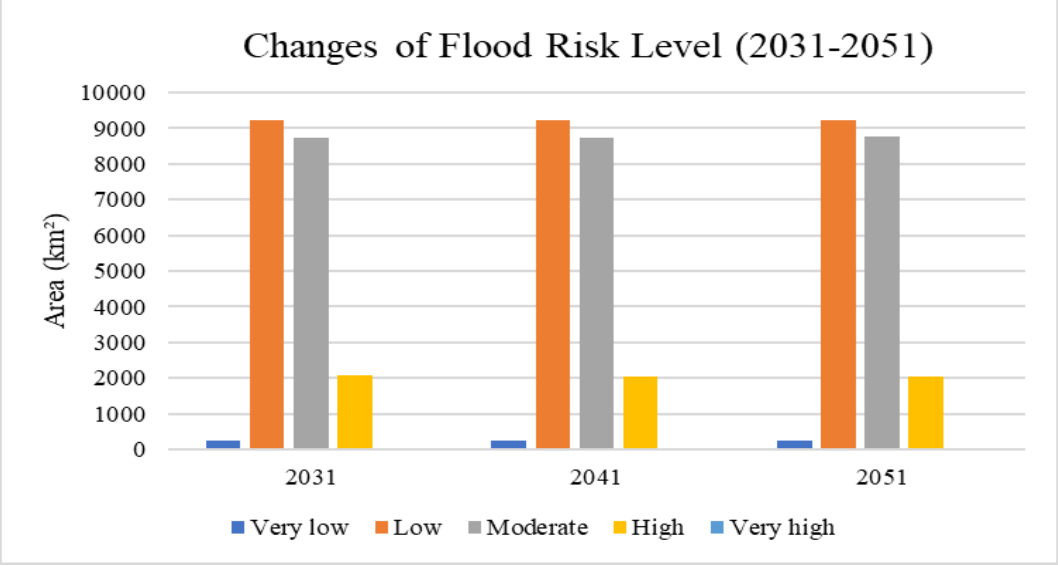

FIGURE 4.15. Changes of the flood risk level for 2031, 2041 and 2051

4.4.3 Analysis of Flood Risk Map

The flood risk maps were created using thematic mapping and AHP. It was then categorized using the natural break method in the ArcGIS environment, displaying five major flood risk classes, ranging from very low to very high.

By referring to the results obtained from Table 4.10 and 4.11, the outcomes show that the area of very low flood risk level (Level 1) increase from 227.36 km^2 to 278.36 km^2 during 2001 until 2011. Then the area experienced decrease to 245.26 km^2 during 2021. Next, the area of low flood risk level (Level 2) increase from 9027.04 km^2 to 9183.31 km^2 during 2001 until 2011 which continuously increase to 9213.70 km^2 during 2021. While for the moderate flood risk level (Level 3), it shows that there is a slight increase of area from 8763.33 km^2 to 8783.95 km^2 during 2001 until 2011 then decrease to 8721.55 km^2 during 2021. However, for the high flood risk level (Level 4), it appears that there is a significant decrease of area from 2277.38 km^2 to 2062.50 km^2 during 2001 until 2011 then during 2021, the area increase to 2101.57 km^2. Finally, for the very high flood risk level (Level 5), the change of area seems to be in the same trend as Level 4. There is a small decrease of area from 48.84 km^2 to 43.41 km^2 during 2001 until 2011 then during 2021, the area increase to 47.75 km^2.

As for the prediction of flood risk maps in the year 2031 until 2051, the results can be found in Table 4.12 and Table 4.13. The results reveals that the area of very low flood risk level (Level 1) experienced a minor decrease from 238.75 km^2 to 237.67 km^2 during 2031 until 2041. For the year 2041 until 2051, the result presents that there is no changes in the area for Level 1 flood. Then, the area of low flood risk level (Level 2) increase from 9220.22 km^2 to 9239.75 km^2 during 2031 until 2041 which will be continuously increase to 9244.63 km^2 during 2051. While for the moderate flood risk level (Level 3), it indicates that there is a slight decrease of area from 8751.39 km^2 to 8749.76 km^2 during 2031 until 2041 then a little increase to 8755.73 km^2 during 2051. Whereas for the high flood risk level (Level 4), there will be a continuous decrease in the area from 2074.98 km^2, 2057.62 km^2 to 2050.02 km^2 throughout 2031, 2041 and 2051, respectively. Lastly, for the very high flood risk level (Level 5), the area is expected to be increase a bit from 44.49 km^2 to 45.04 km^2 during 2031 until 2041 then during 2051, the area decrease to 41.78 km^2.

The spatial distribution of flood events at Perak which has been classified into five

risk level are shown in Figure 4.13 (a), (b) and (c) for 2001 – 2021, and Figure 4.14 (a), (b) and (c) for 2031 – 2051. From the results, it can be concluded that the flood occurrence for all the flood risk level happened in the same area of distribution throughout 2001 – 2051. The very low and low flood risk level (Level 1 and 2) are found in the North and North-East side of Perak. This includes Hulu Perak, east side of Larut and Matang, Selama, Kuala Kangsar, east side of Kinta and Batang Padang. The area has less rainfall intensity, high drainage density and TWI. The elevation is very high while the slope is very steep as the areas are noticeably located at mountainous region and are mostly covered with vegetation or forest. Hence, the flood risk level at these areas are low.

The moderate flood risk level (Level 3) are found mostly at West side until South part of Perak which are Kerian, Larut and Matang, Manjung, Perak Tengah, Hilir Perak, Kinta, Batang Padang and central part of Kuala Kangsar. From the land use classification, it can be observed that the area is mainly consist of agricultural lands, and the wetness level is moderately high due to the plantation purpose. The rainfall intensity and drainage density are fairly distributed within these areas. Moreover, the areas are at low elevation and the surface from ground level is very gentle.

The high and very high flood risk level (Level 4 and 5) are identified at South part of Perak particularly at Manjung, Perak Tengah and Hilir Perak. These areas have high rainfall intensity. Although there are high drainage density, these areas are close to the river and remarkably situated at developed land that has low elevation and the surface from ground level is very gentle. Thus, the flood risk level at these areas increased.

CHAPTER 5

CONCLUSION AND RECOMMENDATION

This study successfully investigate the flood causative factors for Perak state which are rainfall intensity, drainage density, topographic wetness index, slope, elevation, land use, normalized difference vegetation index and soil types.

The ANN-CA model has been effectively created for the prediction of land use changes for Perak. The findings of this study reveals that urban areas will grew rapidly and have a significant rise, by 4555.10 km^2 to 4980.42 km^2, for 2031 – 2051. Moreover, the barren lands will also experience some increase in the areas. The expansion in the land use changes for urban areas and barren lands might be due to the expected growth in commercial, residential, and industrial areas. However, the forest in Perak will encounter degradation in the area from 15087.61 km^2 to 14795.43 km^2, for 2031 – 2051. Minimal decreases were revealed in the classes of water bodies and agricultural lands.

Next, the relative importance of the flood causative factors have been compared in a pairwise comparison matrix to gain the weight values during the process of AHP. To accomplish the objective of this study, AHP-GIS was used as spatial forecasting tools to map the flood risk areas in Perak according to their weights. Based on the results, the high and very high flood risk level were identified in the South-West part of Perak particularly at Manjung, Perak Tengah and Hilir Perak.

As for the recommendations, additional parameters that influenced the land use changes such as aspect, distance from the road and population density, can be used as spatial input variables when training the ANN model to get more accurate prediction result. Next, the validation of flood risk map can be done by using Area Under the Curve (AUC) method to verify the accuracy of the AHP-GIS model.

REFERENCES

Arslan, M., Roxin, A. M., Cruz, C., Ginhac, D. (2017). A review on applications of big data for disaster management, in: 2017 13th International Conference on Signal-Image Technology & Internet-Based Systems (SITIS), IEEE, pp. 370–375, https://doi.org/10.1109/SITIS.2017.67.

Arun, R., & Premalatha, K. (2020). Flood Damage Assessment Using Remote Sensing And GIS: The Past and Present. International Journal of Civil Engineering and Technology (IJCIET), 11*(12),* 1-5. doi: 10.34218/IJCIET.11.12.2020.001

Asian Development Bank. (2013). The rise of natural disasters in Asia and the Pacific: Learning from ADB's experience Mandaluyong City, Philippines. *Independent Evaluation ADB.*

Asokan, A., & Nakulraj, K.R. (2020). Predicting Flood Using Artificial Neural Networks. *International Journal of Applied Engineering Research, 15,* 53-57.

Cao, C., Xu, P., Wang, Y., Chen, J., Zheng, L., & Niu, C. (2016). Flash Flood Hazard Susceptibility Mapping Using Frequency Ratio and Statistical Index Methods in Coalmine Subsidence Areas. *Sustainability*, *8*(9), 948. https://www.mdpi.com/2071-1050/8/9/948

Crabbé, A. H., Cahy, T., Somers, B., Verbeke, L.P., Van Coillie, F. (2020). Neural Network MLPClassifier (Version 2.18.25) [QGIS]. https://bitbucket.org/kul-reseco/lnns.

Dang, N. M., Babel, M. S., & Luong, H. T. (2011). Evaluation of food risk parameters in the Day River Flood Diversion Area, Red River Delta, Vietnam. Natural Hazards, 56(1), 169-194. doi:10.1007/s11069-010-9558-x

Dano, U.L., Balogun, A.L., Matori, A.N., Wan Yusouf, K., Abubakar, I.R., Said Mohamed, M.A., Aina, Y.A., & Pradhan, B. (2019). Flood Susceptibility Mapping Using GIS-Based Analytic Network Process: A Case Study of Perlis, Malaysia. Water, 11(3), 615. https://doi.org/10.3390/w11030615

Department of Irrigation and Drainage. (2020). Laporan Banjir Tahunan 2019. *Pusat Ramalan dan Amaran Banjir Negara (PRABN) Bahagian Pengurusan Sumber Air Dan Hidrologi, Jabatan Pengairan Dan Saliran, Malaysia.*

Dung, N. B., Minh, D. T., Long, N. Q., & Ha, L. T. T. (2020). Weights Of Factors Contributing To Flood Formation In The Lam River Basin, Vietnam. Journal Of Southwest Jiaotong University, 55(2). doi:10.35741/issn.0258-2724.55.2.50

Earth Explorer. (n.d.). USGS Science for a Changing World. https://earthexplorer.usgs.gov/

Elsafi, S.H. (2014). Artificial Neural Networks (ANNs) for flood forecasting at Dongola Station in the River Nile, Sudan. *Alexandria Engineering Journal*, *53*(3), 655-662. doi.org/10.1016/j.aej.2014.06.010.

Elsheikh, R.F.A., Ouerghi, S., & Elhag, A.R. (2015). Flood Risk Map Based on GIS, and Multi Criteria Techniques (Case Study Terengganu Malaysia). Journal of Geographic Information System, 7, 348-357. 10.4236/jgis.2015.74027.

FAO-UNESCO Soil Map of the World. (2022). Food and Agriculture Organizations of the United Nations, FAO Map Catalog. https://data.apps.fao.org/map/catalog/srv/eng/catalog.search#/metadata/446ed430-8383-11db-b9b2-000d939bc5d8

Fei, L., Shuwen, Z., Jiuchun, Y., Liping, C., Haijuan, Y., & Kun, B. (2018). Effects of land use change on ecosystem services value in West Jilin since the reform and opening of China. Ecosystem Services, 31(A), 12–20. https://doi.org/10.1016/j.ecoser.2018.03.009

Goepel, K. D. (2018). Implementation of an Online Software Tool for the Analytic Hierarchy Process (AHP-OS). International Journal of the Analytic Hierarchy Process, 10(3). https://doi.org/10.13033/ijahp.v10i3.590

Gopal, S. (2017). Artificial neural networks in geospatial analysis. The International Encyclopedia of Geography. https://doi.org/10.1002/9781118786352.wbieg0322

Guerra, F., Puig, H., & Chaume, R. (1998). The forest-savanna dynamics from multi-date Landsat-TM data in Sierra Parima, Venezuela. International Journal of Remote Sensing, 19(11), 2061–2075. https://doi.org/10.1080/014311698214866

Helmer, E.H., Brown, S., & Cohen, W.B. (2000). Mapping montane tropical forest successional stage and land use with multi-date Landsat imagery. International Journal of Remote Sensing, 21(11), 2163–2183. https://doi.org/10.1080/01431160050029495

Hernandez, J. F., Aguilera, G. D., Gonzalvez, P. R., Taboada J. M. (2015). Image-based modelling from unmanned aerial vehicle (UAV) photogrammetry: an effective, low-cost tool for archaeological applications, Archaeometry 57 128–145, https://doi.org/10.1111/ arcm.12078.

Hijmans, R. (n.d.). Data-Interpolating Variational Analysis, DIVA-GIS Free Spatial Data. https://www.diva-gis.org/gdata

Jain, S., Singh, R., & Seth, S. (2000). Design flood estimation using GIS supported GIUHApproach. Water Resources Management, 14, 369-376. doi:10.1023/A:1011147623014

Jat, M.K., Garg, P., & Khare, D. (2008). Monitoring and modelling of urban sprawl using remote sensing and GIS techniques. International Journal of Applied Earth Observation and Geoinformation, 10(1), 26–43. https://doi.org/10.1016/j.jag.2007.04.002

Kamarudin N.K. (2020). Spatial Modelling of Flood Susceptibility in Perlis Using Geographic Information System (GIS) And Support Vector Machine (SVM).

Khoirunisa, N., Ku, C.-Y., & Liu, C.-Y. (2021). A GIS-Based Artificial Neural Network Model for Flood Susceptibility Assessment. *International Journal of Environmental Research and Public Health, 18*(3). doi.org/10.3390/ijerph18031072

Kia, M.B., Pirasteh, S., Pradhan, B., Mahmud, A.R., Sulaiman, W.N.A., & Moradi, A. (2012). An artificial neural network model for flood simulation using GIS: Johor River Basin, Malaysia. *Environmental Earth Sciences, 67*(1), 251–264. doi:10.1007/s12665-011-1504-z

Koem, C. (2020). Flash flood hazard mapping based on AHP with GIS and satellite information in Kampong Speu Province, Cambodia. International Journal of Disaster Resilience in the Built Environment, 12*(5)*, 457-470. doi: 10.1108/IJDRBE-09-2020-0099

Li, X., & Yeh, A.G. (2002). Neural-network-based cellular automata for simulating multiple land use changes using GIS. International Journal of Geographical Information Science, 16(4), 323-343. https://doi.org/10.1080/13658810210137004

Looi, S. (2014, December 28). Perak Tengah District the Worst Hit with 3,882 Flood Victims. *New Straits Times.* Retrieved from https://www.nst.com.my/news/2015/09/perak-tengah-district-worst-hit-3882 flood-victims

López, E., Bocco, G., Mendoza, M., & Duhau, E. (2001). Predicting land-cover and land-use change in the urban fringe: A case in Morelia city, Mexico. Landscape and Urban Planning, 55(4), 271–285. https://doi.org/10.1016/S0169-2046(01)00160-8

Lu, D., Mausel, P., Brondizio, E., & Moran, E. (2004). Change detection techniques. International Journal of Remote Sensing, 25(12), 2365–2401. https://doi.org/10.1080/0143116031000139863

Luu, C., Von Meding, J. & Kanjanabootra, S. (2017). Assessing flood hazard using flood marks and analytic hierarchy process approach: a case study for the 2013 flood event in Quang Nam, Vietnam. Natural Hazards, 90(3), 1031-1050.

Mandviwala, M. D., Joshi, G. S., & Prakash, I. (2016). Assessment Of Impact Of The Flood Causative Factors For Flood Vulnerability In Lower Tapi River Basin UsingGIS And Remote Sensing. National Conference on Water Resources & Flood Management with special reference to Flood Modelling October 14-15, 2016, SVNIT SuratAt: Surat, India.

Munawar, H.S., Hammad, A.W.A., & Waller, S.T. (2021). A review on flood management technologies related to image processing and machine learning. *Automation in Construction, 132.* doi.org/10.1016/j.autcon.2021.103916

Munir, S.N.U., Sidek, L.M., Haron, S.H., Noh N.S.M., Basri, H., Marufuzzaman, M., Hafiz, Z.M., & Razad A.Z.A. (2018). Flood Frequency Analysis at the Downstream of Sg. Perak River Basin using Annual Maximum Flow Discharge Data. *International Journal of Engineering & Technology, 7*(4), 709-712. doi:10.14419/ijet.v7i4.35.23094

Ogato, G. S., Bantider, A., Abebe, K., & Geneletti, D. (2020). Geographic information system (GIS)-Based multicriteria analysis of flooding hazard and risk in Ambo Town and its watershed, West shoa zone, oromia regional State, Ethiopia. *Journal of Hydrology: Regional Studies,* 27. doi:https://doi.org/10.1016/j.ejrh.2019.100659

Opolot, E. (2013). Application of Remote Sensing and Geographical Information Systems in Flood Management: A Review. *Research Journal of Applied Sciences, Engineering and Technology, 6,* 1884-1894. doi:10.19026/rjaset.6.3920

Pijanowski, B.C., Tayyebi, A., Doucette, J., Pekin, B.K., Braun, D., Plourde, J. (2014). A big data urban growth simulation at a national scale: configuring the GIS and neural network-based land transformation model to run in a high-performance computing (HPC) environment. Environmental Modelling Software, 51, 250-268.

Pradhan, B. (2009). Flood susceptible mapping and risk area delineation using logistic regression, GIS and remote sensing. *Journal of Spatial Hydrology, 9*(2), 1-18.

Prediction Of Worldwide Energy Resource, POWER (2021). Data Access Viewer v2.0.0, National Aeronautics and Space Administration (NASA) Langley Research Center (LaRC). https://power.larc.nasa.gov/data-access-viewer/

Roy, A., & Inamdar, A.B. (2019). Multi-temporal Land Use Land Cover (LULC) change analysis of a dry semi-arid river basin in western India following a robust multi-sensor satellite image calibration strategy. Heliyon, 5(4), e01478. https://doi.org/10.1016/j.heliyon.2019.e01478

Saaty, T.L. (1980). The Analytical Hierarchy Process, Planning, Priority, Resource Allocation; RWS Publications: Pittsburgh, PA, USA, 1980.

Sharir, K., Rodeano, R., & Mariappan, S. (2019). Flood Susceptibility Analysis (FSA) Using Analytical Hierarchy Process (AHP) Model at The Kg. Kolopis area, Penampang, Sabah, Malaysia. Journal of Physics: Conference Series, 1358 012065. doi: 10.1088/1742-6596/1358/1/012065

Singh, A. (2010). Review Article Digital change detection techniques using remotely sensed data. International Journal of Remote Sensing, 10(6), 989–1003. https://doi.org/10.1080/01431168908903939

Sulaiman, N.A., Mastor, T.A., Mat, M.S.C., & Samad, A.M. (2015). Flood hazard zoning and risk assessment for Bandar Segamat sustainability using analytical hierarchy process (AHP). 2015 IEEE 11th International Colloquium on Signal Processing & Its Applications (CSPA), 72-77, doi: 10.1109/CSPA.2015.7225621.

Szwagrzyk, M., Kaim, D., Price, B., Wypych, A., Grabska, E., & Kozak, J. (2018). Impact of forecasted land use changes on flood risk in the Polish Carpathians. Nat Hazards, 94, 227–240. https://doi.org/10.1007/s11069-018-3384-y

Thanh, L.N., & De Smedt, F. (2011). Application of an analytical hierarchical process approach for landslide susceptibility mapping in a luoi district, thua thien hue province, Vietnam. Environmental Earth Sciences, 66(7), 1739-1752.

Tayyebi, A., Pijanowski, B.C., Linderman, M., & Gratton, C. (2014b). Comparing three global parametric and local non-parametric models to simulate land use change in diverse areas of the world. Environ Model Softw. 59, 202-221. doi :10.1016/j.envsoft.2014.05.022

Tayyebi, A., Tayyebi, A.H., & Khanna, N. (2014c). Assessing uncertainty dimensions in land-use change models: using swap and multiplicative error models for injecting attribute and positional errors in spatial data. International Journal of Remote Sensing, 35, 149-170. doi: 10.1080/01431161.2013.866293

Ullah, K., & Zhang, J. (2020). GIS-based flood hazard mapping using relative frequency ratio method: A case study of Panjkora River Basin, eastern Hindu Kush, Pakistan. *Plos ONE 15*(3): e0229153.doi.org/10.1371/journal.pone.0229153

Wang, L., Chen, D., Liu, Z., Dou, M., Chen, J., & Li, H. (2013). Natural disaster monitoring with wireless sensor networks: A case study of data-intensive applications upon low-cost scalable systems. Mobile Networks and Application, 18(5), 651–663. https://doi.org/10.1007/s11036-013-0456-9

Wedajo, G.K. (2017). LiDAR DEM data for flood mapping and assessment; opportunities and challenges: a review. Journal of Remote Sensing & GIS, 6(4), 2015–2018. https://doi. org/10.4172/2469-4134.1000211.

Witherow, M.A., Sazara, C., Winter, A.I.M., Elbakary, M.I., Cetin, M., & Iftekharuddin, K.M. (2019). Floodwater detection on roadways from crowdsourced images. Computer Methods in Biomechanics and Biomedical Engineering: Imaging & Visualization 7(5-6), 529–540. https://doi.org/10.1080/ 21681163.2018.1488223.

World Health Organization. (n.d.). *Health Topic: Floods.* https://www.who.int/health-topics/floods#tab=tab_1

Yang, X., Chen, R., & Zheng, X.Q. (2016) Simulating land use change by integrating ANN-CA model and landscape pattern indices. Geomatics, Natural Hazards and Risk, 7(3), 918-932. doi: 10.1080/19475705.2014.1001797

Yu, P.S., Yang, T.S., Chen, S.Y., Kuo, C.M., & Tseng, H.W. (2017). Comparison of random forests and support vector machine for real-time radar-derived rainfall forecasting, Journal of Hydrology, 552, 92–104, https://doi.org/10.1016/j.jhydrol.2017.06.020.

Zeshan, M.T., Mustafa, M.R.U., & Baig, M.F. (2021). Monitoring Land Use Changes and Their Future Prospects Using GIS and ANN-CA for Perak River Basin, Malaysia. *Water 2021, 13,* 2286. https:// doi.org/10.3390/w13162286

Zhang, Q., Jindapetch, N., Buranapanichkit, D. (2019). Investigation of image edge detection techniques-based flood monitoring in real-time. IEEE, 2019 16th International Conference on Electrical Engineering/Electronics, Computer, Telecommunications and Information Technology (ECTI-CON), 927–930, https://doi.org/10.1109/ECTI-CON47248.2019.8955273.

Zou, Q., Zhou, J., Zhou, C., Song, L., Guo, J., & Liu, L. (2012). The practical research on flood risk analysis based on IIOSM and fuzzy α-cut technique. Applied Mathematical Modelling, 36(7), 3271–3282. https://doi.org/10.1016/j.apm.2011.10.008.

APPENDICES

APPENDIX A. Average monthly rainfall data for year 2010 – 2020

Station no.	Station name	Longitude	Latitude	Rainfall (mm)
3814158	Sg. Bil	101.4994	3.8186	180.62
3814159	Sg. Slim	101.4086	3.8257	180.62
3814160	Ulu Slim	101.4972	3.8967	180.62
3901001	Changkat Jong	101.1151	3.9866	180.62
3907103	JPS. Bagan Datoh	100.7653	3.9882	181.49
3913148	Kg. Klah Baru	101.3324	3.9812	180.62
4010098	Hospital Telok Intan	101.0227	4.0309	180.62
4011144	Rumah JPS Chui Chak	101.1714	4.0418	180.62
4109094	Kg. Gajah	100.9419	4.1848	180.62
4207048	Pejabat JPS Sitiawan	100.6999	4.2186	181.49
4209093	JPS. Telok Sena	100.8995	4.2556	187.96
4312001	Kg Sahom	101.2152	4.3862	177.80
4411120	Gua Tempurung di Gopeng	101.1898	4.4343	177.80
4205101	Pulau Pangkor	100.5621	4.2066	181.49
4409092	Sg. Perak di Parit	100.9054	4.4722	187.96
4511111	Politeknik Ungku Omar	101.1228	4.5879	177.80
4911077	Sg. Plus di Kg. Lintang	101.1004	4.9400	172.10
4809001	Jambatan Iskandar	100.9717	4.8193	172.10
4807016	Bkt. Larut di Taiping	100.8359	4.8512	173.53
4907020	Batu 14 Batu Kurau	100.7794	4.9778	173.53
5006180	Bkt. Merah	100.6546	5.0310	173.53
5005005	Sungai Samagagah	100.5373	5.0667	173.53
5003028	Stn. Petak Ujian Tg. Piandang	100.3846	5.0700	173.53
5108005	Ibu Bekalan Ulu Ijok	100.8056	5.1224	173.53
5210069	Stn. Pemeriksaan Hutan Lawin	101.0574	5.2977	174.06
5411066	Kuala Kenderong	101.1549	5.4160	174.06
5513001	Tasik Banding	101.3531	5.5502	174.06
5610063	Kg. Lalang di Grik	101.0683	5.6041	174.06

APPENDIX B. Sensitivity score of each factor

Factor	Class	Score
Rainfall	172 – 175 mm	1 (Very Low Risk)
	175 – 178 mm	2 (Low Risk)
	178 -181 mm	3 (Moderate Risk)
	181 – 184 mm	4 (High Risk)
	184 – 187 mm	5 (Very High Risk)
Drainage density	0 – 10.32 km^2	1 (Very Low Risk)
	10.33 – 18.62 km^2	2 (Low Risk)
	18.63 – 26.48 km^2	3 (Moderate Risk)
	26.49 – 35 km^2	4 (High Risk)
	35.01 – 57.22 km^2	5 (Very High Risk)
TWI	2.11 – 5.58	1 (Very Low Risk)
	5.58 – 6.97	2 (Low Risk)
	6.97 – 8.75	3 (Moderate Risk)
	8.75 – 11.22	4 (High Risk)
	11.22 – 21.79	5 (Very High Risk)
Land use	Forest	4 (High Risk)
	Agricultural lands	4 (High Risk)
	Water bodies	5 (Very High Risk)
	Urban areas	1 (Very Low Risk)
	Barren lands	3 (Moderate Risk)
NDVI	Water areas	5 (Very High Risk)
	Urban and Barren lands	4 (High Risk)
	Shrubs	3 (Moderate Risk)
	Unhealthy vegetation	2 (Low Risk)
	Healthy vegetation	1 (Very Low Risk)
Elevation	-27 – 196 m	5 (Very High Risk)
	196 – 504 m	4 (High Risk)
	504 – 828 m	3 (Moderate Risk)
	828 – 1203 m	2 (Low Risk)
	1203 – 2168 m	1 (Very Low Risk)

Slope	Very gentle (0 – 5˚)	5 (Very High Risk)
	Gentle (5 – 10˚)	4 (High Risk)
	Moderate (10 – 25˚)	3 (Moderate Risk)
	Steep (25 – 35˚)	2 (Low Risk)
	Very steep (>35˚)	1 (Very Low Risk)
Soil types	Orthic Acrisol	1 (Very Low Risk)
	Eutric Gleysols	5 (Very High Risk)
	Dystric Hystosols	4 (High Risk)
	Ferric Acrisol	1 (Very Low Risk)
	Lithosols	2 (Low Risk)
	Thionic Fluvisols	3 (Moderate Risk)
	Eutric Fluvisols	3 (Moderate Risk)